AD-767 662

EFFECTS OF STRONG EXPLOSIONS. VI. (SOVIET LITERATURE TRANSLATIONS)

Simon Kassel

RAND Corporation

Prepared for:

Advanced Research Projects Agency

December 1972

DISTRIBUTED BY:

NTIS

National Technical Information Service
U. S. DEPARTMENT OF COMMERCE
5285 Port Royal Road, Springfield Va. 22151

ARPA ORDER NO.: 189-1

R-760/5-ARPA
December 1972

AD 767662

EFFECTS OF STRONG EXPLOSIONS-VI
(Soviet Literature Translations)

Compiled by Simon Kassel

A Report prepared for

ADVANCED RESEARCH PROJECTS AGENCY

Reproduced by
NATIONAL TECHNICAL
INFORMATION SERVICE
US Department of Commerce
Springfield, VA. 22151

Rand
SANTA MONICA, CA. 90406

125

ARPA ORDER NO.: 189-1

R-760/5-ARPA
December 1972

EFFECTS OF STRONG EXPLOSIONS-VI (Soviet Literature Translations)

Compiled by Simon Kassel

A Report prepared for

ADVANCED RESEARCH PROJECTS AGENCY

Rand
SANTA MONICA, CA. 90406

APPROVED FOR PUBLIC RELEASE; DISTRIBUTION UNLIMITED

Published by The Rand Corporation

PREFACE

This Report is one in a series entitled "Effects of Strong Explosions" and intended to provide an overview of current Soviet research activities in that field. It falls within the scope of a continuing program, sponsored by the Defense Advanced Research Projects Agency, which undertakes the systematic coverage of selected areas of Soviet scientific and technological literature.

The effects of strong explosions, particularly nuclear explosions, and their simulation under laboratory and field conditions involve a very broad range of phenomena and parameters such as high temperatures, pressures, electromagnetic energy densities, interaction of energy with materials, shock waves in gases, liquids, and solids, and, in general, events occurring under conditions of a high degree of mechanical, thermal, and radiation stress. The series of Rand Reports of which this is the sixth to be published will cover a variety of the pertinent topics as they are reflected in the currently available Soviet literature, by supplying abstracts from and summaries of the scientific and technological publications of the USSR.

The material in the present Report is derived exclusively from Soviet technical writings that, with a few exceptions, appeared in 1971 and 1972. The input material has been reviewed by Rand, and items have been selected for abstracting. The abstracts were prepared by Informatics, Inc., Washington, D.C. They have been arranged by the compiler according to fairly general subject areas, and vary in length depending on the pertinence and significance of the individual papers.

The information assembled in this Report covers our most recent knowledge of Soviet research on the effects of explosions, and should prove useful to American scientists working in this and related fields of research.

CONTENTS

KEY TO JOURNAL ABBREVIATIONS

DAN SSSR	Doklady Akademii Nauk SSSR (Reports of the Academy of Sciences USSR)
FGiV	Fizika goreniya i vzryva (Physics of Combustion and Explosion)
FIKhOM	Fizika i khimiya obrabotki materialov (Physics and Chemistry of Materials Processing)
F-KhMM	Fiziko-khimicheskaya mekhanika materialov (Physico-Chemical Mechanics of Materials)
FTT	Fizika tverdogo tela (Solid-State Physics)
GiA	Geomagnetizm i aeronomiya (Geomagnetism and Aeronomy)
IAN B	Akademiya nauk Belorusskoy SSR. Izvestiya. Seriya fiziko-matematicheskikh nauk (Academy of Sciences, Belorussian SSR. News. Series on Physico-Mathematical Sciences)
IAN Uzb.	Akademiya nauk Uzbekskoy SSR. Izvestiya. Seriya fiziko-matematicheskikh nauk (Academy of Sciences, Uzbek SSR. News. Series on Physico-Mathematical Sciences)
I-FZh	Inzhernerno-fizicheskiy zhurnal (Engineering Physics Journal)
IVUZ Avia.	Izvestiya vysshikh uchebnykh zavedeniy. Aviatsiya. (IVUZ, Aviation)
MP	Mekhanika polimerov (Polymer Mechanics)
MTT	Akademiya nauk SSSR. Izvestiya. Mekhanika tverdogo tela (Academy of Sciences, USSR. News. Solid State Mechanics)
MZhIG	Mekhanika zhidkosti i gaza (Mechanics of Liquid and Gas)
OiS	Optiko i spektroskopiya (Optics and Spectroscopy)
OMP	Optiko-mekhanicheskaya promyshlennost' (Optico-Mechanical Industry)

Preceding page blank

RZhF	Referativnyy Zhurnal. Fizika (Abstracting Journal, Physics)
RZhKh	Referativnyy Zhurnal. Khimiya (Abstracting Journal, Chemistry)
RZhMekh	Referativnyy Zhurnal, Mekhanika (Abstracting Journal, Mechanics)
TVT	Teplofizika vysokikh temperatur (High-Temperature Thermophysics)
ZhETF	Zhurnal eksperimental'noy i teoreticheskoy fiziki (Journal of Experimental and Theoretical Physics)
ZhPMTF	Zhurnal prikladnoy mekhaniki i tekhnicheskoy fiziki (Journal of Applied Mechanics and Technical Physics)
ZhPS	Zhurnal prikladnoy spektroskopii (Journal of Applied Spectroscopy)
ZhTF	Zhurnal tekhnicheskoy fiziki (Journal of Technical Physics)

I. SHOCK WAVES AND EXPLOSIONS IN GASES

Bayev, V. K., B. N. Kondrikov, V. P. Korobeynikov, V. V. Mitrofanov, R. I. Soloukhin, and M. Ye. Topchiyan. Research on explosion gas dynamics and reacting systems. FGiV, no. 2, 1971, 311-317.

The Third International Colloquium on explosion gas dynamics and reacting systems took place on September 12-17, 1971 in Marseilles, France. Basic topics of theoretical and experimental research reported on were in the field of unsteady dynamic gas flow, accompanied by physicochemical transformations of the medium; gas-dynamic aspects of detonation; and problems of the physics and chemistry of rocket-fuel combustion and working processes in engines. The colloquium also dealt with the gas dynamics of explosions in space. The conference was divided into seven sections: a) space phenomena, b) vortex flow, c) explosion gas dynamics, d) detonation, e) shock waves, f) gas-liquid systems, and g) reacting systems. V. P. Korobeynikov gave a gas-dynamic description of the motion and explosion of meteorites on the basis of the supposed explosion pattern of the Tungusskiy meteorite.

A session on twisted flows included a joint report by four U.S. delegates and V. P. Korobeynikov on the influence of heat conduction and viscosity on wave propagation from a powerful explosion. A. A. Vasil'yev, T. P. Gavrilenko, and M. Ye. Topchiyan described planned experimental research on the position of the Chapman-Jouguet plane in a multifront detonation wave in gas. V. P. Korobeynikov, G. G. Chernyy, et al. presented a theoretical analysis and an example of a numerical

calculation of the point initiation of a detonation for the plane, cylindrical, and spherical cases. A report by I. V. Babaytsev, B. N. Kondrikov, and V. F. Tyshevich on low-velocity processes in high density charges described low velocity detonations in cast and pressed materials.

R. I. Soloukhin discussed IR-spectroscopy methods in high-temperature gas dynamics, including applications of emission and absorption IR-spectroscopy in the study of nonequilibrium processes in shock waves. R. Emrich (USA) and R. I. Soloukhin reported on the resonance absorption of 3.39 micron laser radiation by methane molecules in shock wave compressed gas. C. Brochet (France) and R. I. Soloukhin examined the occurrence and location of unstable zones in the chemical reaction behind an incendiary shock wave front.

The 65 papers presented in the colloquium will be published in a special number of the journal of the International Academy of Astronautics, "Astronautica Acta."

Barzykin, V. V., V. A. Veretennikov, Yu. M. Grigor'yev, and A. S. Rozenberg. Results of Third All-Union Symposium on combustion and explosions. FGiV, no. 4, 1971, 616-618.

The Symposium, which took place July 5-10, 1971 in Leningrad, was attended by 730 representatives from 210 organizations. There were three sections: on combustion, detonation, and kinetics. Three plenary reports and 154 section reports were presented. The plenary sessions reports were presented by Ya. B. Zel'dovich, (The contribution of D. A. Frank-Kamenetskiy to the theory of combustion), V. V. Pomerantsev (Atomization, evaporation, and combustion of liquid fuel), and A. D. Margolin (The present status and some problems of the combustion theory of condensed systems).

At the section on combustion, 79 reports were presented in 9 subject areas: ignition in condensed systems, steady combustion of condensed systems, combustion stability and non-steady combustion of condensed systems, combustion in dispersion systems, flame propagation limits in gases, laminar combustion of gases, combustion of organic fuels, turbulent combustion of gases, and combustion in supersonic flow. The problem of supersonic combustion was included for the first time in the program of the All-Union Symposiums.

At the section on detonation, 36 reports were presented in 4 subject areas: detonation of condensed explosives, detonation in gaseous and heterogeneous systems, sensitivity of explosives to mechanical interactions, and physico-chemical transformations of materials from shock wave effects. In addition to reports on the continuation of theoretical and experimental research on shock wave propagation in condensed media, other reports in this section dealt with

the mechanism of physicochemical processes under conditions of shock compression, monomer polymerization, diffusion in a shock-wave front, and polarization of metals and dielectrics. An increasing number of papers discussed precise physical methods for directly observing the property changes of substances under conditions of shock compression.

At the section on kinetics, 39 reports were presented in 8 subject areas: chain reaction kinetics, gas-phase kinetics, elementary processes, kinetics of high temperature processes in shock tubes, kinetics of the thermal decomposition of ammonium perchloride, kinetics of thermal decomposition reactions, kinetic reactions in flames and combustion thermodynamic processes. A. S. Biryukov, A. P. Dronov, Ye. M. Kudryavtsev, G. A. Raynin, and N. N. Sobolev reported on a shock tube investigation of a CO_2 laser.

Alinovskiy, N. I., A. T. Altyntsev, and N. A. Koshilev. Heating of plasma ionic component by a collisionless shock wave. ZhETF, v. 62, no. 6, 1972, 2121-2128.

The energy spectra of plasma ions heated by a collisionless shock wave are obtained by passive corpuscular diagnosis. When an aperiodic shock front with resistive dissipation is formed in the plasma, ion heating appears as a small group of ions (about 10%) with a mean energy of the order of the electron temperature; the remaining ions are cold. Experimental results agree with a theoretical model, in which the origin of this group of particles is explained by the linear Landau damping of ion-acoustic vibrations in resonance ions located in the "tail" of the distribution function, induced in the shock front.

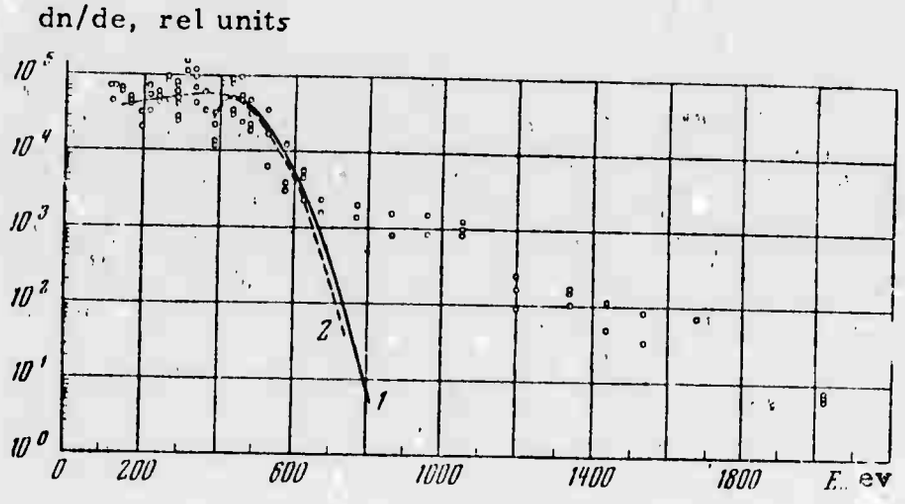

Fig. 1. Typical ion energy spectrum for low Mach numbers ($M < M_{cl}$). Parameters: $M = 1.8$, $h = 2$; $n = 1.4 \times 10^{13}$ cm^{-3}, $H_0 = 520$ oe. 1. Calculated approximation for constant ion velocity, $T_i = 6$ ev, $E_{H\,max} = 4.08$ ev. 2. Calculated approximation for increasing ion velocity, $T_i = 7.5$ ev, $E_{Hmax} = 480$ ev.

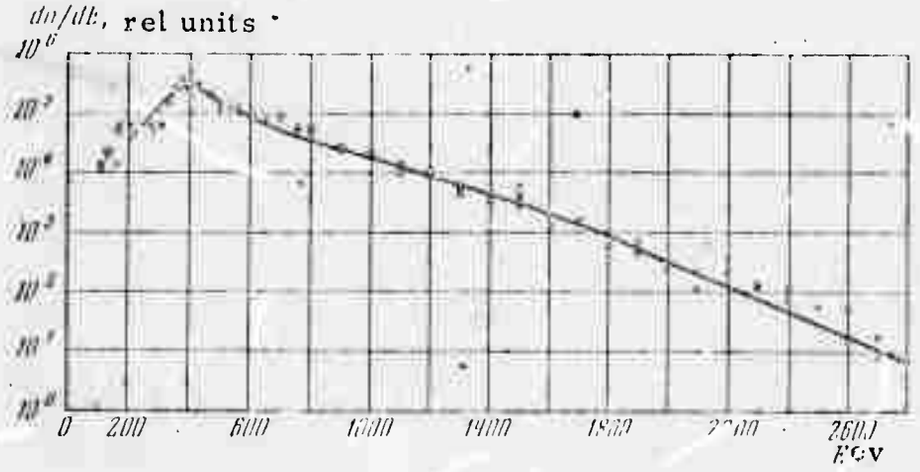

Fig. 2. Typical ion-energy spectrum for the case of $M \gtrsim M_{c2}$. Parameters: $M = 4.5$, $h = 5.4$, $n = 7 \times 10^{13}$ cm^{-3} $H_0 = 280$ oe. Solid line - calculated curve. $T_1 = 12$ ev, $T_2 = 130$ ev, $E_{H\ max} = 380$ ev, $n_2/n_1 \approx 8$.

The main energy content of the plasma is determined by the electron component. Under the conditions of "overturning" of the shock-wave front, predominant heating of the ion component of the plasma is observed, and the ion distribution function is close to an isotropic Maxwell distribution.

Kestenboym, Kh. S., F. D. Turetskaya, L. A. Chudov, and Yu. D. Shevelev. Euler and Lagrange methods for calculations of point explosions in a heterogeneous atmosphere.
IN: Trudy Sektsii po chislennym metodam v gazovoy dinamiki 2-go Mezhdunarodnogo kollokviuma po gazodinamike vzryva i reagiroyushikh sistem, 1969, T. 3. Moscow, 1971, 85-100 (RZhMekh, 5/72, #5B238)

A study is made of a strong point explosion in a nonviscous thermally nonconductive gas. It is assumed that the density and pressure of the atmosphere are altitude-dependent according to an exponential law. Motion is considered in the half plane Π ($r \geq 0$), bounded by the axis of symmetry. The equations of unstabilized motion are written out in terms of Euler and Lagrange coordinates. Region G_0, containing the point in which the explosion occurs, is isolated in half plane π. In solving the problem, the boundary Γ_c (t) of the region is selected in such a manner that within the entire G_0 region, the pressure could be considered constant. The region of difference calculation, G_1, is bounded by the curve $\Gamma_0(t)$, the shock wave front Γ_1 (t), and two segments of the axis of symmetry. The solution of a number of unidimensional problems, including the problem of a point explosion in a homogeneous atmosphere with account taken of counter-pressure, was checked by an applicable method for its verification, good coincidence being obtained with results of the work by D. Ye. Okhotsimskiy, I. L. Kondrashev, Z. P. Vlasov, and R. K. Kazakov (Trudy Matematicheskogo instituta AN SSSR, 1957, 50, 66. RZhMekh, 3/58, #2659). Fairly good correspondence is shown in comparison of the results of calculation of the title problem in terms of Euler and Lagrange variables.

Saltanov, G. A., and L. I. Seleznev.
Variations of flow parameters and flow structure of moist vapor, for the case of interphase heat and mass exchange in the relaxation zone behind a shock wavefront. TVT, no. 6, 1971, 1200-1206.

Relaxation phenomena behind a stationary shock wavefront in moist vapor are analyzed, with allowance for relatively low concentrations of spontaneously condensed fine drops and in the absence of gliding phase motion. The numerical solution of a set of equations of motion determined the flow parameters (p, T, c), flow structure (particle-size distribution), and shock wave width for the thermodynamic equilibrium of a two-phase medium ahead of the shock wave. Theoretical data were found to be in good qualitative agreement with the experiment, e.g. using a Laval nozzle.

II. SHOCK WAVES IN SOLIDS

Andreyev, V. G. and P. I. Ulyakov. Finite dimension volumetric thermal shock in a transparent plate. I-FZh, v. 23, no. 1, 1972, 158-159.

The presence of high temperature gradients during a short-term thermal shock requires the application of a hyperbolic equation of thermal conductivity, which takes into account the finite heat propagation velocity (HPV). In dielectrics, the thermal conductivity of the lattice is the basic mechanism of heat transfer, and the HPV equals the velocity of sound c_0 in the medium. The movement of temperature and stress perturbations with equal velocity along a material signifies the propagation of a single wave. When the given initial conditions are discrete (instantaneous shock), the pressure, amplitude, and density in such a wave undergo a shock, and equations of thermal elasticity are inapplicable for finding the parameters of the medium during a rupture of its continuity.

In real processes, thermal shock has a finite duration, and stress accretion takes place continuously behind the wave leading edge. In the present work, the solution of the dynamic problem of thermal elasticity for a three-dimensional shock of finite duration is obtained by the method of Laplace transforms. Expressions are obtained for the temperatures and stresses, and the problem is solved in parallel with the parabolic equation of thermal conductivity. The quasi-static stressed state is a particular case (when $c_0 \rightarrow \infty$). Introducing heat-propagation velocity equal to sound velocity into the thermoelasticity problem eliminates the physically contradictory appearance of stresses prior to wave arrival at a given point. Analysis shows that the amplitude of the

temperature front attenuates exponentially with time and does not affect the stress wave motion. After passage of the elastic-wave front, a field of quasi-static stresses is established.

Boyko, M. M., V. A. Letyagin, and V. S. Solov'yev. Experimental investigation of shock wave attenuation in steel. ZhPMTF, no. 2, 1972, 101-104.

Shock wave attenuation in steel specimens from the contact blast of a plane-wave trotyl charge, with a 50 mm diameter and 10 mm height, was studied experimentally. Monotonic attenuation of the maximum shock-compression pressure was observed at increasing distances from the contact surface. Shock wave attenuation was caused by a relief wave which overtook the shock waves from the direction of the charge. The propagation rates of the primary and secondary shock waves were computed using the known shock-wave velocity and the experimentally obtained time intervals between the emergence of the waves to the free surface of variable thickness plates. The experiments show that up to a thickness of $x_1/h \approx 1.35$ (x_1, specimen thickness; h, charge height) the shock waves propagated in steel in three stages, and thereafter degenerated into a two-stage form.

Zak, M. A. Geometric shock waves in an anisotropic elastic body. MTT, no. 3, 1972, 161-162.

An investigation is made of a quasi-linear hyperbolic system of equations for wave propagation in an elastic anisotropic medium. Surface wave front equations of motion are derived and

resolved with respect to coefficients of the first and second quadratic forms. A formula for the characteristic propagation rate of discontinuities of the surface form was obtained: $\lambda' = \text{grad}\ \lambda \cdot n$, where $\lambda(N_1, N_2, N_3)$ is the characteristic velocity in the direction of normal N with the directional cosines N_1, N_2, N_3; n is the unit vector of the normal of a discontinuity line of the surface form, in a plane tangential to the surface and forming an acute angle to the main normal. It is shown that if the line of discontinuity of the wave-front shape is an asymptotic curve, the discontinuities of the geodesic curvature of this curve are distributed at a constant rate; $\lambda'' = \text{grad}\ \lambda \cdot \tau$, where τ is the unit vector of a tangent to the discontinuity line, with unit vectors τ, M, n forming a right triangle. However, if the shape discontinuity line is not asymptotic, then $\lambda'' = 0$.

Investigation of the initial wave propagation equations in integral form permitted establishment of the propagation rate of fracture lines of a "ridge" type on the wave-front surface, and fracture points of a "peak" type on the discontinuity lines of the wave-front surface shape. The propagation rates coincide with the characteristic rates λ' and λ'', if the values of the discontinuities are infinitely small, but differ from them if the discontinuity values are finite.

It is shown that the characteristic velocities λ' and λ'' generally depend on those shape parameters which transport the weak discontinuities. This leads to the possibility of the formation of ridges and peaks, propagating in the form of shock waves at the rate $\lambda+'$ and $\lambda\ +''$ as a result of "accumulation" of the corresponding shape discontinuities, which are weaker than the discontinuities at the crests and peaks. It is emphasized that the shock waves obtained have a purely geometrical sense which characterizes the configuration of that region of the arguments in which movement of the medium is considered.

Khristoforov, B. D. Shock wave parameters for explosion of a spherical charge in porous NaCl. FGiV, no. 4, 1971, 594-599.

Laboratory experiments were conducted to determine the parameters of shock waves in a solid at various porosity values within the range $1 \lesssim \bar{R} \lesssim 9$, where $\bar{R} = R/R_0$ is the ratio of the distance R between the point of measurement and the charge to the charge radius R_0. The effect of rock porosity near an explosion on the explosion parameters in the medium was considered. NaCl powder with a grain size of about 0.3 mm was used to simulate the properties of natural rock. The powder was pressed to densities of $\rho_{00} = 2.12$, 1.87, and 1.72 g/cm^3, and the single-crystal density was $\rho_0 = 2.16$ g/cm^3. The porosity of the pressed specimens, defined by the ratio $\eta = 1 - \rho_{00}/\rho_0$, was 2, 13.5, and 20%. The shock-wave parameters were measured by an electromagnetic method proposed by Ye. K. Zavoyskiy. Results show that the porosity of the medium substantially affects the energy dissipation and the shock-wave parameters in the near explosion zone.

Khristoforov, B. D., Ye. E. Goller, A. Ya. Sidorin, and L. D. Livash. Manganin sensor for measuring shock wave pressure in solids. FGiV, no. 4, 1971, 613-615.

A manganin sensor and circuitry are described for recording plane shock wave pressure in a solid within the range 1 to 10^2 kbar. The plane shock wave in the specimen is actuated by a detonation lens (1, Fig. 1) and explosive charge (2). Variation of the charge density and the introduction

of layers of inert materials (3) between the charge and the specimen (4) permit shock wave pressure to be varied within wide limits. A cellophane film (5) protects the sensor wire (6) from deformations resulting from destruction of the specimen. Simultaneously, the pressure in the film, equal to the normal stress in the specimen, is established in about 0.2 microsecond. This is determined by a multiple of the time of passage of the wave along the film thickness. The static and dynamic sensitivity coefficients of the sensor were determined. The dynamic sensitivity coefficient was based on a comparison with results of electromagnetic measurements of shock-wave parameters in NaCl within the range of 3 to 50 kbar and during phase transition in KBr. Electromagnetic measurement data show that in a phase transition in KBr: $u = 0.30 \pm 0.01$ km/sec, $N = 2.60 \pm 0.05$ km/sec; and $p = 21$ kbar. Under these conditions $S = 2.8 \times 10^{-3}$ kbar^{-1}. Values of $S = 2.5$, 2.8, and 3×10^{-3} kbar^{-1} were determined in NaCl specimens with $\rho_0 = 1.88$ g/cm^3 at pressures of 3.5, 6.4, 8.5, and 50 kbar. The dynamic sensitivity coefficient therefore exceeds the static coefficient. In the range above 6 kbar, the dynamic coefficient also increases with pressure in contrast to the static coefficient. This divergence is apparently due to differences in the stressed state of the manganin under two types of loading.

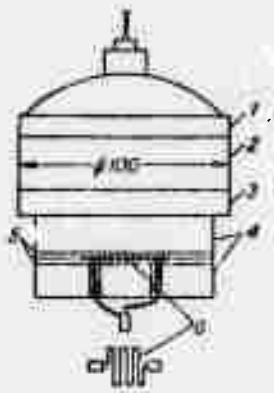

Fig. 1. Diagram of detonator and sensor

III. SHOCK WAVES IN LIQUIDS

Andriankin, E. I., V. K. Bobolev, and A. V. Dubovik. Collapse of an elliptic cavity and explosive initiation in a liquid layer under shock effect. ZhPMTF, no. 5, 1971; 78-85.

Analytical and experimental results are given on the effect of shock excitation of a combustible liquid volume. Criteria are developed for the threshold conditions under which a nominally spherical fluid volume shifts to an elliptical form, and on further compression develops into a cumulative jet; in the limit this results in detonation from adiabatic heating of gas evolved in the volume. Test data on shock generation of jets in liquid nitroglycerine are included, and show qualitative agreement with theoretical results.

Shtessel', E. A., K. B. Pribytkova, and A. G. Merzhanov. A numerical solution to the problem of a thermal explosion with free convection taken into account. FGiV, no. 2, 1971, 167-178.

The authors cite previous works in which the effect of free convection on a gas explosion process is expressed in terms of the Rayleigh (Ra) and Frank-Kamenetsky (δ) criteria. The analysis is extended here to the case of liquid fuel combustion, and is presented as a supplement to earlier experimental work by Merzhanov and Shtessel' (FGiV, no. 1, 1971) in which an empirical correlation between Ra and δ was obtained. The model used assumes an ideal stationary fluid in a uniform semi-infinite vessel; gas evolution is neglected. The results are shown graphically, indicating the conditions under which convection will or will not affect the detonation process.

IV. INTERACTION OF SHOCK WAVES WITH SOLIDS

Batsanov, S. S., Ye. V. Dulepov, E. M. Moroz, L. V. Lukina, and V. V. Roman'kov. Effect of explosions on materials. Shock compression of rare earth metal fluorides. FGiV, no. 2, 1971, 266-269.

Results of a study of shock compression of ten rare earth metal (REM) fluorides and yttrium fluoride are presented. It is shown that the greatest physical characteristics change occurs using 30-50 g hexogene charges, with the exception of CeF_3 and PrF_3 for which the most significant changes occur using 100-150 g charges. All the shock-compressed materials displayed optical anisotropy, since the initial materials were finely dispersed and therefore were pseudoisotropic. The new phase is normally inhomogeneous, and the properties change occurs (or accumulates) in different grains with varying intensity; the value of the effect is maximal only in a small number of crystalline particles. Table 1 shows refractivity indices of the new phases;

a	b			c		
	d_4^{25}, g/cm³	•	n_D	d_4^{25}, g/cm³	•	n_D
LaF_3	5.87	13.7	1.60	5.87	14.5	1.57
CeF_3	6.03	14.1	1.61	5.79	16.2	1.58
PrF_3	6.09	14.8	1.62	5.90	21.0	1.58
NdF_3	6.17	16.0	1.60	5.84	22.0	1.58
$SmF_3+0,5\,H_2O$	5.75	16.0	1.60	6.47	16.6	1.57
EuF_3	6.76	11.7	1.58	6.73	13.2	1.68
GdF_3	6.87	10.8	1.58	6.78	12.0	1.56
TbF_3	6.78	12.2	1.58	6.45	13.7	1.54
DyF_3	7.21	10.8	1.58	7.00	11.7	1.53
HoF_3	7.44	10.6	1.58	7.39	11.0	1.54
YF_3	5.02	11.2	1.56	4.90	11.7	1.53*

Table 1. a - compound, b - initial material, c - compressed material

measurement precision by the immersion method is ± 0.003, with results rounded to the second decimal place. An exception is EuF_3.

The compressed REM fluorides density decrease was generally due to the formation of internal defects. For a partial phase transition from the rhombic modification to the hexagonal, which should be accompanied by a density increase, the formation of imperfections also brings about a EuF_3 specimen density decrease. The dielectric permeability increased but in a different manner after shock compression. This increase was primarily caused by the appearance of defects. No marked changes of electrical conductivity due to the shock compression were observed. The conductivity was ionic in all cases, reflecting the absence of surface imperfections. Shock-compressed fluorides of La, Ce, Pr, Nd, Gd, Dy, and Y manifested no changes in atomic structure, but polymorphic conversions were observed in Sm, Ho and Eu fluorides. In the case of EuF_3 an inverse phase transition occurred in the form of increased hexagonal modification. Comparative data show that temperature is not the only determining factor in the stabilization of this modification.

V. HIGH-SPEED FLOW PAST BODIES

Bezmenov, V. Ya., and P. I. Gorenbukh. Application of a nonstationary analogy to an investigation of explosive wave effects on an obstacle in a hypersonic tunnel. Uchenyye zapiski Tsentral'nogo aerodinamicheskogo instituta, v. 2, no. 6, 1971, 48-54. (RZhMekh, 5/72, no. 5V282)

The results are presented of an experimental investigation of shock wave interaction from a blunt body (a plate with a blunt leading edge), with a solid boundary (a plate with a sharp leading edge), in a helium stream at M = 23 to 27. The pressure distribution around the plate with the sharp leading edge behind the incident shock wave is given. By means of a detonation analogy, the results obtained are used to analyze the effect of a plane shock wave on a two-dimensional barrier. It is shown that in this case the experimental results agreed with the calculated data. Counterpressure was not taken into account during the tests.

Tsvetkova, M. V. Characteristics of supersonic flow around blunt bodies under conditions of intensive injection. IN: Trudy II Respublikanskoy konferentsii po aerogidromekhanike, teploobmenu i massoobmenu. Sektsiya "Aerodinamika bol'shikh skorostey". Kiyev, Kiyevskiy universitet, 1971, 112-115. (RZhMekh, 5/72, no. 5B415)

Results are presented of experimental research on the effect of air injection through a permeable body surface on the position and

shape of the shock wave, the surface pressure distribution, and the wave resistance of the body. The research was performed on a cylinder with spherical bluntness, and on a truncated cone with a developing break. The surface porosity was 60%, the Mach numbers were M = 3-5, and the relative flow rate of the injected gas was varied within the limits of 0 to 1.0. Two experimental regimes were established: a regime with moderate injection intensity (relative flow rate less than 0.2) and a regime of "strong" injection (flow rate greater than 0.2). In the moderate flow regime, a sharp change of the flow characteristics takes place as the rate is increased (increased resistance, shock-wave separation, and increased angle of shock-wave incidence). The flow calculation can therefore be conducted on the basis of boundary-layer theory, taking viscous interaction into account. The regime of "strong" injection is characterized by the presence of a boundary "blow-off" region of the boundary layer. In this case the flow parameters cannot be determined on the basis of boundary-layer theory.

Biberman, L. M., S. Ya. Bronin, and A. N. Lagar'kov. Heating and flow around blunt bodies during atmospheric entry. IN: Trudy Sektsii po chislennym metodam v gazovoy dinamike 2-go Mezhdunarodnogo kollokviuma po gazodinamike vzryva i reagiruyushchikh sistem, 1969, Moskva, v. 3, 1971, 134-153. (RZhMekh, 5/72, no. 5B424)

The problem of the aerodynamic heating of blunt bodies entering the atmosphere at velocities higher than parabolic is considered. A detailed justification is given of the theoretical assumptions, permitting an efficient solution to the problem of determining the total heat flux at the

critical point of a blunt body. Thus, for hypersonic flight velocities, the assumption of small width of the shock layer in comparison to a characteristic dimension of the body is valid. It becomes possible to describe the flow distribution near the critical point by systems of ordinary differential equations. Considerations are presented for disregarding the viscous structure of the shock wave so that the problem is solved without separating the shock layer into a nonviscous region and a boundary layer. It is noted that the final expression for the total heat flux at the critical point contains only values obtained from the solution to the "nonviscous" problem with allowance for gas radiation in the shock wave, as well as other values from the solution to the "viscous" problem, but with radiation ignored. An iteration method is used to solve the integro-differential system of equations. Graphic results are presented of computer--aided calculations of the relationships of the total heat flux and its convective and radiant components owing to variation of the flight velocities (to 20 km/sec) and the nose curvature radius at the critical point.

Sil'vestrov, V. V., and V. P. Urushkin. Method for determining density of high speed gas jets. IN: Dinamika sploshnoy sredy. Novosibirsk, no. 7, 1971, 125-129. (RZhMekh, 5/72, no. 5B477)

A method is proposed for determining the density of gas jets moving at a speed of 8-12 km/sec. The jets are formed from the detonation of an explosive in a channel. The method is based on an experimentally obtained law of the motion of a propelled body, using a steel ball. The successive positions of the ball in a chamber are recorded by x-ray pulse photography. The characteristics of the x-ray facility

were such that the minimum size of the steel ball was 2 mm. The proposed method made it possible to determine the boundaries of the potential values and the characteristics of the three-dimensional distribution of the gas-jet density with an error of 8-10%. A significant nonuniformity of density distribution of the cross section and jet length was revealed. The maximum value of gas density attained was 0.2-0.23 g/cm^3.

Davlet-Kil'deyev, R. Z. Heat and flow characteristics of a body of revolution in a supersonic gas flow. IN: Uchenyye zapiski Tsentral'nogo aero-gidrodinamicheskogo instituta, v. 2, no. 6, 1971, 103-107. (RZhMekh, 5/72, no. 5B556)

The results are presented of an experimental investigation of flow and heat on the surface of a conic nose cylinder with a half-angle of 13.5°. Tests were carried out in a thermal wind tunnel at angles of attack $\alpha = 0^\circ$, 10°, and 20°, $N = 5$, and $R_\infty = 10^7\ m^{-1}$. The heat flow was measured by the method of heat-indicating coatings; the flow pattern was determined on the basis of washed-out points and the results of heat transfer measurements. At $\alpha = 0^\circ$ and 10°, the heat flow agreed with calculations for laminar flow; the flow around the body was detached. At $\alpha = 20^\circ$ the flow became detached and a zone of increased heat fluxes appeared on the lee surface. Two three-dimensional expanding funnel-shaped vortices simultaneously appeared above the zone.

Turanov, Ye. N. Heat evolution at a concave surface in supersonic flow. IN: Trudy II Respublikanskoy konferentsii po aerogidromekhanike, teploobmenu i massoobmenu. Sektsiya "Aerodinamika bol'shikh skorostey". Kiyev. Kiyevskiy universitet, 1971, 168-172. (RZhMekh, 5/72, no. 5B998)

Heat exchange on the concave frontal surfaces of axisymmetric bodies was investigated at Mach numbers M = 2.5, 3.0, and 3.5. The concave surface was spherical and varied in depth from 0 to R, where R is the radius of the maximum cross section of the body. The shock wave in front of the concave body pulsated at a frequency of 1 kHz. The heat exchange on the axis of symmetry of the concave surface was on the same order as that on the surface of the flat face. Tests were also conducted on models with through apertures in the concave surface. At the relative aperture area of 6-10%, the pulsations ceased. The heat flux at the critical point in this area was less than at the critical point of a flat face and varied approximately in accordance with a linear law as a function of cavity depth.

Pavlov, B. M. Solution to complete Navier-Stokes equations in problems on flow around blunt bodies. IN: Trudy sektsii po chislennym metodam v gazovoy dinamiki 2-go Mezhdunarodnogo kollokviuma po gazodinamike vzryva i reagiruyushchikh sistem, 1969. Moskva; v. 1, 1971, 55-66. (RZhMekh, 5/72, no. 5B887)

Numerical solutions to complete Navier-Stokes equations are obtained for problems of the flow and heat exchange of a viscous gas

around various bodies (a sphere, a right circular cylinder, an ellipsoid, a hyperboloid of revolution, and a blunt cone) for Reynolds numbers $R \leq 10^3$ and Mach numbers $2 \leq M_\infty \leq 15$. Calculation results revealed a weak upstream transmission of the perturbation; this permitted calculation of the flow field on the windward side of the body in the stream independently of the flow on the lee side. The solutions are sought using an explicit difference scheme by the method of adjustments. The density, pressure, and heat flow characteristics, the resistance coefficients, and the position of the shock wave and of the sonic line are listed for various values of R and M. Good agreement with experimental data for $R>10$ is indicated.

Stulov, V. P., G. F. Telenin, and L. I. Turchak. Supersonic flow around blunt bodies by various gas mixtures with high speed chemical reactions. IN: Trudy sektsii po chislennym metodam v gazovoy dinamiki 2-go Mezhdunarodnogo kollokviuma po gazodinamike vzryva i reagiruyushchikh sistem, 1969. Moskva, v. 3, 1971, 3-28. (RZhMekh, 5/72, no. 5B1114)

A numerical method is proposed for the calculation of flow near the frontal part of axisymmetric blunt bodies in various gas mixtures, undergoing nonequilibrium chemical processes. Underlying the method is the notion that the total system of the equations of relaxation gas dynamics is divided into two systems, one of which (the equations of motion) is solved by the conventional method, while an implicit difference scheme along the streamline is used for solving the relaxation equations. The problem is solved by iteration between the systems at each calculated layer. The proposed method makes it possible to investigate flow with an arbitrary degree of unevenness. The calculations assume that the hypersonic flow around the body.

was at a zero angle of attack and that a separation shock wave is formed in front of it. All the internal degrees of freedom of the gas-mixture particles, including the oscillatory degrees are considered to reach equilibrium at the shock-wave front. The calculation results are presented graphically.

Air flow in a blunt sphere was investigated under conditions in which only oxygen dissociation was significant in the chemical reactions. The validity of binary similarity (similarity of flow at a constant product of the characteristic linear dimension on the free-stream density) was verified under a wide range of conditions. A justification is given for the selected physicochemical model of air for the given range of free-stream parameters (M = 8 to 15). Consideration is given to the nonequilibrium flow of a mixture of carbon dioxide, nitrogen, and argon. A strong dependence of the flow upon the initial concentrations of the mixture components is shown. The regularity of flow transition to equilibrium is verified. Questions on selection of the physicochemical model and the kinetics of a given mixture are analyzed.

Perminov, V. D., and Ye. Ye. Solodkin. Axisymmetric bodies with minimum resistance at a specific heat flow to the surface. IN: Uchenyye zapiski Tsentral'nogo aero-gidrodinamicheskogo instituta, v. 2, no. 6, 1971, 32-40. (RZhMekh, 5/72, no. 5B345)

For axisymmetric bodies with a flat leading edge and a mildly sloping lateral surface, an approximate solution is given to a variational problem of the shape of a body of minimal resistance in a hypersonic gas under a specific total heat flow to the surface. A modified Newtonian formula is used for calculation of the pressure distribution. The formulated isoperimetric problem of the shape of an axisymmetric body of given dimensions with a flat leading edge, and minimum resistance at a given total heat flux, is solved numerically by a modified method of local variations at values of $M_\infty = 6$, 10, and 30, and $R_O = 10^6$. It is shown that, under the specified conditions, the requirements of minimal resistance and minimal heat flow to the body surface are contradictory.

Popov, F. D., and I. M. Breyev. Calculation of supersonic flow around blunt bodies by the finite-difference method. IN: Trudy II Respublikanskoy konferentsii po aerogidromekhanike, teploobmenu i massoobmenu. Sektsiya "Aerodinamika bol'shikh skorostey". Kiyev, Kiyevskiy universitet, 1971, 50-55. (RZhMekh, 5/72, no. 5B336)

A finite-difference scheme is proposed for the calculation of static, mixed, axisymmetric flow over the nose section of a blunt body in a supersonic ideal gas. The shock layer considered is transformed

into a rectangular region, a difference grid is introduced, and the equations of the problem are represented in difference form with second-order of accuracy. The system of nonlinear difference equations is solved by the method of successive approximations. Each iteration deals with a system of linear equations, to which the method of successive elimination is applied. In contrast to the numerical method of Babenko, et al. (Babenko, Voskresenskiy, Lyubimov, and Rusanov . Prostranstvennoye obtekaniye gladkikh tel ideal'nym gazom. Three-dimensional flow around smooth bodies by an ideal gas . Moskva, Nauka, 1964, RZhMekh, 1965, 4B207K), the system of difference equations in the iteration process is not broken down into equations along individual radial lines, but is solved simultaneously for the entire region. The method of successive matrix elimination is also generalized for the case of cell matrices. Damping is used to accelerate iteration convergence. Some calculation results are presented to illustrate the convergence of the numerical solution.

Molodtsov, V. K., and A. N. Tolstykh.
Calculation of supersonic viscous flow around blunt bodies. IN: Trudy Sektsii po chislennym metodam v gazovoy dinamike 2-go Mezhdunarodnogo kollokviuma po gazodinamike vzryva i reagiruyushchikh sistem, Moskva, v. 1, 1971, 37-54. (RZhMekh, 5/72, no. 5B335)

Supplementary results are presented to calculations using Navier-Stokes equations of hypersonic flow around a spherically blunt model by methods proposed earlier by the authors (Tolstykh, A. ZhVMMF, no. 1, 1966, 113-120, RZhMekh, 1966, 8B257; Molodtsov, ZhVMMF, no. 9, 1969, 1211-1217, RZhMekh, 1970, 2B384). The calculations were for $M_\infty = 10$ and various Reynolds numbers, and a temperature factor and index ω within the law of the relationship of the viscosity coefficient to temperature,

$\mu \sim T^{\omega}$. A brief analysis is given of the calculation results (presented in 10 figures), as well as a comparison with experimental and other theoretical data.

Kukarkina, M. A., and Yu. B. Radvogin. Application of a divergent scheme for solution of flow problems. Trudy II Respublikanskoy konferentsii po aerogidromekhanike, teploobmenu i massoobmenu. Sektsiya "Aerodinamika bol'shikh skorostey". Kiyev. Kiyevskiy universitet, 1971, 66-72. (RZhMekh, 5/72, no. 5B334)

A modification is proposed of a known method of calculating supersonic gas flow (Babenko, Voskresenskiy, Lyubimov, and Rusanov. Prostranstvennoye obtekaniye gladkikh tel ideal'nym gazom. Three-dimensional flow around smooth bodies by an ideal gas . Moskva, Nauka, 1964. RZhMekh, 1965, 4B207K). The modified equations of gas dynamics are written in divergent form and in a conversion to new independent variables which permit the interval length of the difference grid, in terms of physical units, to be decreased without difficulty in regions of acute change of the parameters. Examples of flow around two complex bodies at M = 10 show that the method may be used for the calculation of flow with large gradients of gas-dynamic values.

Katskova, O. N., and P. I. Chushkin. Three-dimensional supersonic flow around bodies by a gas with nonequilibrium physico-chemical transformations. IN: Trudy II Respublikanskoy konferentsii po aerogidromekhanike, teploobmenu i massoobmenu. Sektsiya "Aerodinamika bol'shikh skorostey". Kiyev. Kiyevskiy Universitet, 1971, 63-69. (RZhMekh, 5/72, no. 5B332)

A scheme proposed earlier by the authors is applied to the investigation of supersonic nonequilibrium flow in a three-dimensional nozzle and near the tail section of a blunt body in the shape of an inverted cone. The numerical scheme is obtained by representing the relationships of the desired functions to the angular variable ψ of a cylindrical system of coordinates by trigonometric polynomials along ψ with interpolation points on a series of meridional planes ψ = const. For determination of the desired functions, an approximating system of differential equations of two independent variables is consequently obtained on all the meridional planes of interpolation. At supersonic speeds this system is hyperbolic, with two sets of wave characteristics (Mach lines) and a family of flow-line analogs on each interpolation plane, and is solved by an inverse scheme of the method of characteristics. Calculation is performed in accordance with layers of x = const, where x is measured along the axis of the cylindrical system of coordinates.

The calculated examples are of nonequilibrium flow of dissociated oxygen. The nozzle had a cylindrical external generatrix of elliptical cross section, as well as an elliptical (narrowing) central body. The calculations revealed a "freezing" of the gas composition during expansion in the nozzle. In calculating nonequilibrium flow around a blunt body with a tail section in the shape of an inverted cone, various half-angles of the cone, $\omega = 0^{\circ}$, 10°, and 30°, and two angles of attack $\alpha = 10^{\circ}$ and 15°, were considered. It is noted that nonequilibrium oxygen dissociation causes a

significant temperature drop and a density increase in comparison to the case of a perfect gas. The simultaneous effect of disequilibrium on pressure and, consequently, on the aerodynamic characteristics of the investigated bodies is slight. It was established that the gas composition near the body surface on the conical tail section becomes practically frozen.

Bulakh, B. M. Vortex interaction of a three-dimensional laminar boundary layer on a circular cone with external nonviscous supersonic flow. IN: Materialy nauchno-tekhnicheskoy konferentsii Leningradskogo instituta svyazi. Leningrad, no. 4, 1971, 146-147. (RZhMekh, 5/72, no. 5B329)

The velocity, pressure, density, and temperature components in a laminar boundary layer flowing around a cone at an angle of attack are represented in the form of expansions into a power series on the basis of the small parameter $\epsilon = R - \frac{1}{2}$, where R is the Reynolds number. The initial terms of the expansions describe a self-similar solution to a problem of the boundary layer on the cone; the coefficients of the second term take into account the boundary layer interaction with a nonviscous eddy flow outside the boundary layer. Corrections to the solution associated with this interaction may in some instances be 10% or higher.

Balakin, V. B., and V. V. Bulanov. Numerical solution to a problem on shock wave interaction with a cylinder in supersonic flow. I-FZh, v. 21, no. 6, 1971, 1033-1039. (RZhMekh, 5/72, no. 5B327)

A difference scheme of a second order of exactness is proposed for the calculation of the axisymmetric unsteady flow of an ideal gas. A numerical solution is obtained to the problem of a shock wave impacting a cylinder in supersonic flow. In the first stage of solution, the problem of streamline flow is solved by the method of adjustment. In the second stage the problem of shock interaction is solved. Pulsed pressure values were calculated for regimes with Mach numbers within the range of 1.5 to 5.

Antonova, A. M. High speed gas flow around a slender three-dimensional body. Trudy II Respublikanskoy konferentsii po aerogidromekhanike, teploobmenu i massoobmenu. Sektsiya "Aerodinamika bol'shikh skorostey". Kiyev, Kiyevskiy universitet, 1971, 99-102. (RZhMekh, 5/72, no. 5B340)

A formulation of the problem of flow around a slender body by a hypersonic gas is described. Within hypersonic theory of small perturbations, the problem can be reduced to the solution of a quasi-linear second-order equation in terms of partial derivatives of the hyperbolic type for a flow function in a plane of similarity variables. An iteration method of solving a Cauchy problem for this equation is proposed which reduces to an inverse problem for the flow around a slendor pointed body with an attached shock wave.

Vasil'yev, M. M. Supersonic flow around a cone at an angle of attack. Trudy II Respublikanskoy konferentsii po aerogidromekhanike, teploobmenu i massoobmenu. Sektsiya "Aerodinamika bol'shikh skorostey". Kiyev. Kiyevskiy universitet, 1971, 75-78. (RZhMekh, 5/72, no. 5B338)

The method reported earlier by the author (MZhiG, no. 1, 1970, 33-39, RZhMekh, 1970, 6B240) is used to solve the problem of supersonic flow around a cone at an angle of attack with an accuracy to values of the second order of smallness, inclusively. The results are compared with a solution of the problem by a method of nets of Babenko, et al. (Babenko, Voskresenskiy, Lyubimov, and Rusanov. (Prostranstvennoye obtekaniye gladkikh tel ideal'nym gazom. Three-dimensional flow around smooth bodies by an ideal gas). Moskva, Nauka, 1964, RZhMekh, 1965, 4B207K), and with the solution obtained by the method of expansion into a double series by Sapunov(IN: Transzvukovyye techeniya gaza. Transonic gas flow. Saratov. Saratovskiy universitet, 1964, 164-177, RZhMekh, 1965, 9B231).

Kosorukov, A. L. Supersonic flow around smooth bodies with relaxation. IN: Trudy II Respublikanskoy konferentsii po aerogidromekhanike, teploobmenu i massoobmenu. Sektsiya "Aerodinamika bol'shikh skorostey". Kiyev. Kiyevskiy universitet, 1971, 70-74. (RZhMekh, 5/72, no. 5B337)

Steady flow around an axisymmetric blunt body by a nonviscous, nonthermally conductive gas is solved by the method of adjustments, with account taken of oscillatory relaxation. To reduce the difficulties of solving relaxation equations, the author divides the initial system into two subsystems: 1) equations for the velocity and pressure components, and

Vasil'yev, M. M. Supersonic flow around a cone at an angle of attack. Trudy II Respublikanskoy konferentsii po aerogidromekhanike, teploobmenu i massoobmenu. Sektsiya "Aerodinamika bol'shikh skorostey". Kiyev. Kiyevskiy universitet, 1971, 75-78. (RZhMekh, 5/72, no. 5B338)

The method reported earlier by the author (MZhiG, no. 1, 1970, 33-39, RZhMekh, 1970, 6B240) is used to solve the problem of supersonic flow around a cone at an angle of attack with an accuracy to values of the second order of smallness, inclusively. The results are compared with a solution of the problem by a method of nets of Babenko, et al. (Babenko, Voskresenskiy, Lyubimov, and Rusanov. (Prostranstvennoye obtekaniye gladkikh tel ideal'nym gazom. Three-dimensional flow around smooth bodies by an ideal gas). Moskva, Nauka, 1964, RZhMekh, 1965, 4B207K), and with the solution obtained by the method of expansion into a double series by Sapunov(IN: Transzvukovyye techeniya gaza. Transonic gas flow. Saratov. Saratovskiy universitet, 1964, 164-177, RZhMekh, 1965, 9B231).

Kosorukov, A. L. Supersonic flow around smooth bodies with relaxation. IN: Trudy II Respublikanskoy konferentsii po aerogidromekhanike, teploobmenu i massoobmenu. Sektsiya "Aerodinamika bol'shikh skorostey". Kiyev. Kiyevskiy universitet, 1971, 70-74. (RZhMekh, 5/72, no. 5B337)

Steady flow around an axisymmetric blunt body by a nonviscous, nonthermally conductive gas is solved by the method of adjustments, with account taken of oscillatory relaxation. To reduce the difficulties of solving relaxation equations, the author divides the initial system into two subsystems:. 1) equations for the velocity and pressure components, and

2) equations for the temperature and the oscillatory energy. The first system of equations is solved by the Euler method. In the second system the free term is dependent on the desired values, and the nonlinear difference equations obtained are solved by the Newton method. The method contains two iteration processes. Flow of the mixture 0_2, N_2, and Ar (air) around a sphere and ellipsoids is calculated for various initial conditions.

Maykapar, G. I. Calculating the resistance of a body on the basis of the shape of the bow shock wave. IN: Uchenyye zapiski Tsentral'nogo aerogidrodinamicheskogo instituta, v. 2, no. 6, 1971, 23-31. (RZhMekh, 5/72, no. 5B344)

Using theorems of the conservation of mass and momentum, an analysis of the order of the magnitudes and the numerical results confirmed the validity of a formula for computing the wave resistance of a semi-infinite cylindrical body based on the shape of the bow shock wave. The formula may be used for determining the resistance of the leading sections of axisymmetric and cylindrical bodies on the basis of flow shadow photography.

Babenko, K. I., V. N. Ivanova, E. P. Kazandzhan, M. A. Kukarkina, and Yu. B. Radvogin. Nonsteady flow around the leading section of a blunt body. IN: Trudy II Respublikanskoy konferentsii po aerogidromekhanike, teploobmenu i massoobmenu. Sektsiya "Aerodinamika bol'shikh skorostey". Kiyev, Kiyevskiy universitet, 1971, 29-43. (RZhMekh, 5/72, no. 5B325)

A numerical solution is given for the problem of supersonic flow around the leading section of a blunt body with a plane of symmetry in inert gas flow. A normalizing system of curvilinear coordinates is used, in which the calculated region has fixed boundaries. A finite-difference method is generalized and developed similar to an established one. The principal variation of the proposed method is associated with calculation of the frontal shock wave and the construction of a well-defined system of difference equations. Finite-difference approximation is employed for the derivatives together with the corresponding equation coefficients. The nonlinear system of difference equations obtained is solved by an iteration method, the complete system being divided into subsystems pertaining to each of the three spatial variables. The indeterminate form of the difference equations on the zero radial line is shown. The algorithm developed is used for the determination of steady supersonic flow around triaxial ellipsoids and ellipsoids of revolution. Results of numerical calculations are presented.

Fedotov, B. N. and G. G. Skiba. Nonstationary three-dimensional motion of bodies of revolution in an ideal gas. IN: Trudy II Respublikanskoy konferentsii po aerogidromekhanike, teploobmenu i massoobmenu. Sektsiya "Aerodinamika bol'shikh skorostey". Kiyev. Kiyevskiy universitet, 1971, 44-49. (RZhMekh, 5/72, no. 5B326)

A boundary-value problem is considered for equations of three-dimensional nonsteady motion with boundary conditions on shock wave and body surfaces. In the selected system of coordinates, the functions characterizing the nonsteady motion of the body are the angle of precession, the angle of nutation, two components of the vector of angular velocity, and the velocity of the origin of coordinates. A sinusoidal relationship of the perturbation functions to time is postulated. The expressions of the fundamental functions are substituted into the initial equations. Linearization led to the reduction of the problem to the solution of a nonlinear system and a series of linear systems with coefficients dependent on the solution to the nonlinear system. A brief description is given of th procedure for solving the three-dimensional boundary-value problem with application to smooth bodies of revolution with spherical bluntness, with oscillations centered in the center of sphere. The scheme of G. F. Telenin, et al. is applied in the regior adjoining a sphere. (Gilinskiy, Telenin, and Tinyakov, IAN SSSR. Mekhanika i mashinostroyeniye, no. 4, 1964, 9-28. RZhMekh, 1965, 5B263), while in the region between the shock wave and a conic surface the difference method of Babenko, et al is applied. (Babenko, Voskresenskiy, Lyubimov, and Rusanov. Prostranstvennoye obtekaniye gladkikh tel ideal'nym gazom. Three-dimensional ideal gas flow around smooth bodies by an ideal gas. Moskva, Nauka, 1964, RZhMekh, 1965, 4B207K).

Kryukova, S. G., and V. S. Nikolayev. Experimental investigation of optimally balanced profiles in viscous supersonic flow. IN: Uchenyye zapiski Tsentral'nogo aero-gidrodinamicheskogo instituta, v. 2, no. 5, 1971, 94-98. (RZhMekh, 5/72, no. 5B377)

The optimal shapes of three classes of profiles with a given location of the balancing center of pressure were investigated in viscous hypersonic flow stream ($M_\infty = 5.2$, $R = 150$). The upper boundary of the quality factor as a function of the location of the center of pressure is found for the profiles under consideration. The experimental results are compared with theoretical data calculated by one of the authors (Nikolayev. Uchenyye zapiski Tsentral'nogo aero-gidrodinamicheskogoinstituta, v. 1, no. 6, 1970, 67-74, RZhMekh, 1971, no. 10B229).

Rakhmatulin, Kh. A., and S. I. Mevlyudov. Supersonic flow around a slender body in a two-phase mixture. IN: Voprosy vychislitel'noy i prikladnoy matematiki, Tashkent, no. 9, 1971, 166-175. (RZhMekh, 5/72, no. 5B1204)

The problem of supersonic flow around a slender profile or body of revolution by a two-phase mixture is considered in an approximation of linear theory. A model of the interpenetrating motion of two or three interacting continuous media (components) is used. Instead of an equation of energy of the gas or mixture, an assumption of barotropicity is used; i.e., the pressure perturbation p is considered to be a known function

of the density perturbation of the mixture

$$\rho = \sum_{n=1}^{N} \rho_n,$$

where ρ_n is the density of the corresponding component, and N is the number of components. In the solution, the entire region of the perturbed flow is divided into two subregions (I) and (II). To subregion (I), bounded by the bow wave (in the linear approximation, by a characteristic curve) and a dividing line (the trajectory of the particles reflected from the leading edge of the body), a two-velocity model is applied. To subregion (II), bounded by the dividing line and the body surface, a three-velocity model is applied, in which the third component is the particles reflected from the body in accordance with the law of specular reflection. Formulas which yield a solution in the indicated regions are presented. When obtaining a solution in region (II), use is made of an expansion into a series along the y coordinate, which is normal to the free-stream flow.

Mevlyudov, S. I. Linear theory of supersonic flow around a slender body in a two-phase mixture. IN: Voprosy vychislitel'noy i prikladnoy matematiki, Tashkent, no. 9, 1971, 156-165. (RZhMekh, 5/72, no. 5B1203)

In a formulation analogous to the preceding work by Rakhmatulin and the author, a linear problem is considered of the flow of a two-phase mixture around a slender two-dimensional or axisymmetric body. The author in this work assumes that the equation

$$\sum_{n=1}^{N} \rho_{n0} \left(\frac{\partial u_n}{\partial y} - \frac{\partial v_n}{\partial x} \right) = 0$$

where u_n and v_n are a projection of the velocity vectors of the corresponding components on the x and y axes; N is the number of components, while ρ_{nO} are unperturbed values of their densities, permitting the flow of each component to be considered irrotational and accordingly the introduction of a perturbation potential for each component. The remainder of the investigation is done using operational calculus methods.

Gadion, V. N., V. G. Ivanov, G. I. Mishin, S. N. Palkin, and L. I. Skurin. Electronic and gas dynamic parameters of hypersonic wakes behind models moving in argon. ZhTF, no. 5, 1972, 1049-1055.

The conductivity, velocity, and width of hypersonic wakes behind models moving in argon were studied within a velocity range of 3300-4900 m/sec, at pressures of 30, 40, 60, 80, and 100 torr and a temperature of about 290° K. The experiments were conducted on polyethylene 8 mm cylindrical models of small elongation with spherical noses and conic skirts. Copperplated aluminum spheres 5.4 mm in diameter were used for control experiments. The models were shot into a pressure chamber provided with instrumentation for measurement of the wake conductivity and velocity. Wake velocity was measured electrodynamically and by the Toepler method.

Measurement results are presented for tests of wake conductivity at a constant pressure and variable velocity or at a constant velocity and variable pressure. The latter test results show that as the distance from the body increases, a relationship develops between the

conductivity σ and the pressure in the mainstream. In the far wake ($x/d > 150$-200, where d is the diameter of the cylindrical part of the model), this relationship approaches

$$\sigma \sim \frac{1}{\sqrt{p_\infty}}$$

Relationships of the electron density drop N_e to the distance along the wake are plotted in terms of x/d. The electron-collision frequencies data were determined taking electron velocity distribution into account.

On the basis of the experimentally obtained initial conditions, changes of the wake temperature, velocity, diameter, and electron concentration are calculated using different models of viscosity. The theoretical and experimental data are compared for a wake sector up to 500 calibers (x/d) in length.

Lobanov, V. F. and Yu. I. Fadeyenko. Calculation of the stresses in an elastic sphere situated in a hypersonic stream. IN: Dinamika sploshnoy sredy, Novosibirsk, no. 7, 1971, 226-232 (RZhMekh, 5/72, #5V285)

An axisymmetric problem is considered, dealing with determination of the stress field originating in a hollow elastic sphere during its presence in a hypersonic stream. The aerodynamic pressure acting upon the sphere is considered to be known and is given in the form of a function that depends upon the angular coordinate in accordance with Newton's law. The inner surface of the sphere is stress-free. The solution is represented in series form using Legendre polynomials. Numerical calculations were conducted on a digital computer for a solid sphere and for a hollow sphere with a Poisson coefficient $m = 2$.

Yermak, Yu. N. and V. Ya. Neyland. The effect of viscosity upon shock wave detachment during flow around a cylinder by a hypersonic stream. Uchenyye zapiski Tsentral'nogo aero-gidrodinamicheskogo institute, v. 2, no. 6, 1971, 41-47. (RZhMekh, 5/72, #5B315)

An investigation is made of the effect of viscosity and thermal conductivity upon detachment of the shock wave from the surface of a circular cylinder in a hypersonic stream of viscous gas, with vertical interaction of the boundary layer with the nonviscous shock layer. It is shown that in distinction from the case of vortical interaction on a sphere, viscosity and thermal conductivity exert a strong influence in this case upon detachment of the shock wave, since the greatest part of the shock-layer thickness consists of a region of slow viscous flow, lying near the surface of the body.

VI. REENTRY SHIELDING

Gashchenko, A. G. Statistical aspects of thermal stability of refractory materials. Problemy prochnosti, no. 5, 1972, 79-82.

On the basis of test data on 60 corundum and 50 zirconium dioxide specimens, it was confirmed that the dispersion of destructive temperature differentials, which characterize the thermal resistance of refractory ceramic materials, is subject to the Weibull distribution. The variance of destructive temperature differential values under identical conditions of thermal loading (Q = const) is higher than the variance of the limit stress values for mechanical loading, and the parameters M in the corresponding distributions may differ significantly. It was found that when investigating ceramic refractory materials, it is preferable to define the parameter m' on the basis of

$$m' = \frac{d_n}{D^*(\lg X)\,2{,}3059}$$

Here d_n is dependent on the number of test specimens; $D^*(\lg X) = \sqrt{D'(\lg X)}$, where $D'(\lg X)$ is the unbiased value dispersion of the logarithm of random value x. This expression most completely depicts the influence of the statistical aspects of the breakdown kinetics.

Tret'yachenko, G. N. and V. K. Fedchuk. Device for investigating destruction of structural elements in supersonic high temperature gas flow containing a controlled amount of abrasive particles. Problemy prochnosti, no. 5, 1972, 112-113.

On the basis of the gas-dynamic test stand of Pisarenko, et al (IN: Termoprochnost' materialov i konstruktivnykh elementov, Kiyev, 1965), a device was developed for studying the destruction processes of aircraft thermal-protection materials and elements, and flow-through parts of high-temperature machines, simulating operational conditions. By means of this device, it is possible to investigate: (1) destruction and crack formation factors in nozzle-insert materials and heat insulation from an unstable thermal stress state, (2) heat-insulation structures, and (3) the effect of gas flow corrosion-erosion action on the process of nozzle-insert breakdown. The device is capable of producing a stream with a temperature T = 1950° K, a velocity of 1160 m/sec, and a flow rate of up to 1 kg/sec.

The apparatus consists of a sectional supersonic nozzle, a high-temperature combustion chamber, two cooling units, a controlled injector of abrasive particles into the gas stream, and measuring and recording instrumentation. The nozzle consists of three sections: subsonic, critical, and supersonic, fitted together into a single unit. Heat-insulation materials can therefore be tested in a supersonic gas stream, and, by replacement of the critical section with a special chamber, nozzle-insert model specimens can also be tested. The specimen insert is placed in a test chamber, in the form of a metal sheath filled with soot for heat insulation. In addition, high-temperature insulation is provided by a MgO layer. The high-temperature oxygen combustion chamber raises the stream temperature to about 2700° K. Compressed air is supplied at 2-3 atm to a

hopper containing the abrasive, which is fed through a screened rotor into a nozzle for injection into the combustion chamber. The abrasive transfer to the nozzle is regulated by the rotor rate.

Device specifications conform to the gas-flow parameters of the basic gas-dynamic test stand: gas consumption, 517 g/sec; fuel consumption, 60 g/sec; oxygen consumption, 100 g/sec; supersonic nozzle entry temperature, 2500° K; pressure, 3 atm, and pressure behind the nozzle, 1 atm. The Laval nozzle has a critical cross section of 33.6 cm^2 (the diameter is correspondingly 65 mm) and an expanding section length of 170 mm, which with an aperture of $2\alpha = 20^\circ$ controls the outlet diameter of 125 mm. Preliminary tests confirmed the feasibility of the following gas-flow parameters: temperature - 1950° K, and velocity - 1160 m/sec, which corresponds to the Mach number M = 1.22.

Rodichev, Yu. M. Factors of weakening of sheet asbotextolite under intense unilateral heating. Problemy prochnosti, no. 5, 1972, 51-53.

Weakening factors of asbotextolite protective coatings were studied at a linear surface temperature increase of the carrier layer, observed during the heating of aerodynamic structures. The tests were conducted on an installation for studying the mechanical properties of heat-resistant plastics under conditions of programmed intensive unilateral heating during bending. Heat was applied by contact using a thin nickel resistance heater. Load application was by flexure. The specimen surface was heated at constant rates of 0.5, 1, 2, and 4°/sec.

The sheet asbotextolite test specimens were 180 mm long and had a thickness (equal to $h_{(\tau)}$ for the carrier layer) of 10 to 52 mm. Flexure loading of the specimens took place when surface $T^* = 1323^{\circ}$ K. The heating time, determined by the heating rate, was 2100, 1050, 525, and 262.5 sec, respectively. Fig. 1 illustrates experimental data on temperature distribution with respect to thickness of the asbotextolite specimens at the instant of loading.

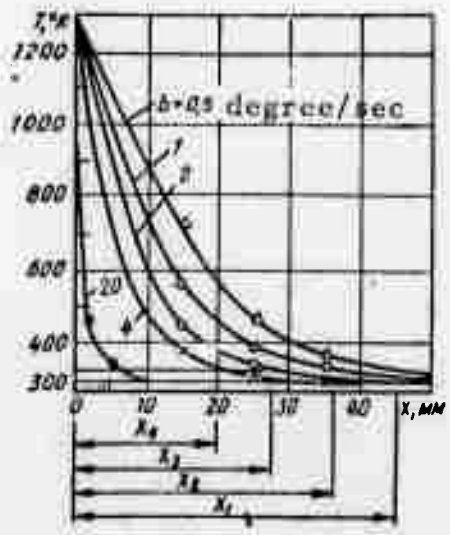

Fig. 1. X_1, X_2, X_3, X_4, -- Materials heating depth of the carrier layer at varying heating rates.

The higher the rate of temperature rise, the greater is the specimen bending strength (Fig. 2). The current thickness of the

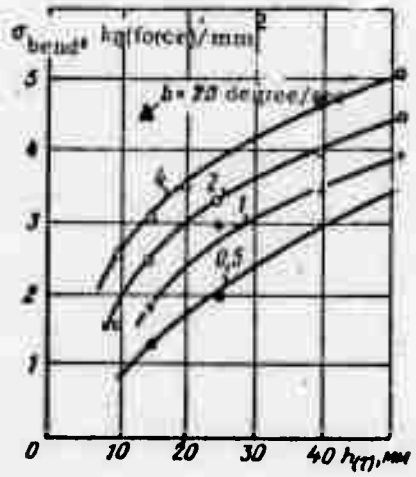

Fig. 2. Bending-strength limit in relation to heating rate and thickness of asbotextolite carrier layer.

carrier layer $h_{(\tau)}$ of coking asbotextolite during unilateral high-temperature heating is also a characteristic factor of its bending strength. With an increase of $h_{(\tau)}$ from 10 to 52 mm, the bending strength limit almost doubles. The greater the specimen thickness, the less is the effect of the heating rate.

These tendencies are a result of an increase in the relative thickness of the carrier layer $\frac{h_{(\tau)}}{X_{(\tau)}}$, where $X_{(\tau)}$ is the heating depth of the carrier layer. Correlation of the obtained characteristics to the value of a Fourier criterion Fo*, which determines the temperature distribution in the carrier layer of the material at the instant of loading under a linear law of temperature change on a heated surface (where a_o

$$Fo^* = \frac{a_0 \tau^*}{h^2_{(\tau)}}, \quad \text{or} \quad Fo^* = \frac{a_0 (T^* - T_0)}{b h^2_{(\tau)}}$$

is the coefficient of temperature conductivity at $T_O = 293^\circ$ K, τ^* is the heating duration, and b is the temperature rise rate on the surface of the carrying portion) permits a relationship to be established between F_O^* and σ_{bend} (the bending strength of the asbotextolite sheet). The required initial thickness of the protective covering can be determined using this relationship and taking the aerodynamic heating conditions into account.

Udovskiy, A. L., N. O. Gusman, and V. N. Barabanov. Effect of test temperature on the energy of destruction of graphite. Problemy prochnosti, no. 5, 1972, 83-84.

To assess the effect of test temperature upon local characteristics of the energy of destruction, bending tests were conducted on specimens of fine-grain, homogeneous 8 x 8 x 40 mm graphite. The graphite was mechanically practically isotropic. The intensity of the elastic deformation energy release (the destruction ductility) was determined within the temperature range 20° to 2000° C. A lateral crack was simulated in each specimen by incision with a fret saw and tapering with a razor blade. The experiment was conducted on a test machine equipped with a low-lag resistance furnace. The high-temperature tests were conducted in an argon atmosphere. In the first stage of operation, at 20° C, the relationship of destruction ductility G to the relative incision size c/d was determined. More than 90 specimens were tested under conditions of

pure flexure. Destruction occurred with negligible brittleness. Load-deflection diagrams were automatically recorded on a two-coordinate potentiometer, and the value of G was computed. In the second stage, tests were conducted at 2000° C. It was found that, at both temperatures within the c/d range from about 0.2 to 0.4, the values of G are invariable and are not a function of the incision depth. G becomes constant at these values of relative incision depth over the entire temperature range from 20 to 2000° C.

Two series of c/d = 0.2 and 0.3 specimens were tested at 500, 1000, 1400, 1800, and 2300° C. Results were used to plot the relationship of the energy of destruction to the test temperature, under the assumption that the critical value of G, $G_c = 2\gamma_{eff}$ (Fig. 1).

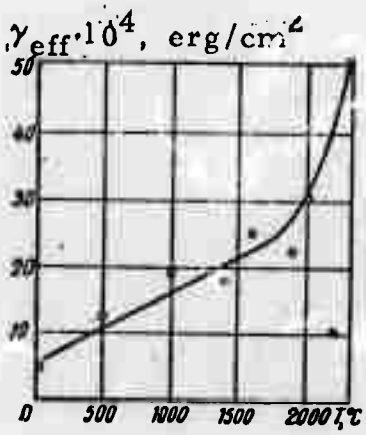

Fig. 1. Destruction energy vs. test temperature.

It was experimentally established that at temperatures of 2000-2300° C the values of γ_{eff} exceed those at 20° C by an order of magnitude. Such a rise in the energy of destruction with an increase of the test temperature is caused by an increase of energy dissipation for plastic deformation at the crack terminus.

Motulevich, V. P., Yu. N. Vorontsov, and V. M. Yeroshenko. Combustion of carbon particles in supersonic flow of a chemically active gas. FGiV, no. 3, 1971, 345-352.

The approximate method of relative correspondence of Motulevich (IFZh, v. 14, no. 1, 1968) is used to evaluate the surface ablation rate on a body purified by a chemically active gas. To check the theoretical relationships of the process, experiments were conducted in a supersonic wind tunnel. Carbon rod models were placed between the nozzle and a cylindrical diffuser 3-4 mm from the nozzle cutoff. The mainstream parameters were: Mach number M = 2.72-3.03, stagnation temperature T_{00} = 1100-1300° K, stagnation pressure p_{∞} = 1.86-2.24 x 10^5 newtons/m^2. The model shapes were a cylinder, a hemisphere-cylinder, and a cone-cylinder. The material nominal density was 1.54 g/cm^3. The model diameter was d = 4-8 mm and relative length was $\overline{l}$ = 6 mm. The modal configuration changes and the surface brightness temperature were measured by photopyrometry. The characteristic wavelength was λ_{eff} = 0.66 microns; the gas was assumed to be optically transparent. The accuracy of temperature measurement was to within ± 4%. When processing the experimental results, it was assumed that the chemical reaction takes place only on the surface within the observed surface-temperature range (1600-2400° K) according to the system:

$$2C+O_2 \rightleftharpoons 2CO.$$

As a result of particle interaction with the flow, the axisymmetric models acquired a shape that can be approximated by an ellipsoid of revolution with the characteristic dimension a = 0.13-2.0. The absolute temperature values near the forward critical point are presented in Table 1.

k_∞	T_{ad}, °K	β, g·cm^{-1}·sec^{-1}	b, g·cm^{-2}sec^{-1}
0,23	1720—1820	0,080—0,120	0,187—0,225
1,0	2050—2250	2,066—0,100	0,39—1,05

Table 1.

Fig. 1 shows that the rate of particle surface change during combustion

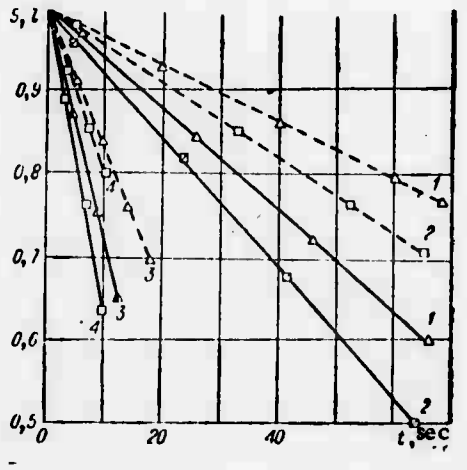

Fig. 1. Change of the relative surface area $\bar{S} = \frac{S}{S_0}$ (S, S_0 are the current and initial values of the model surface area) and the relative length of the model $\bar{l} = \frac{l}{l_0}$ (dotted line) in the combustion process. $k_\infty = 0.23$: 1 - $\bar{a} = 0.3$; 2 - $\bar{a} = 0.7$. $k_\infty \approx 1.00$: 3 - $\bar{a} = 0.2$; 4 - $\bar{a} = 1.4 \div 1.47$.

is linear, irrespective of the value of $\bar{a}$. The mass removal rate at the critical point is also linear. Fig. 2 shows the characteristic experimental

relationships of the mass removal rate from the entire model surface area. The relationship of the total mass removal rate m to the removal rate at the critical point m_o indicates that in the air stream for a particle with $\bar{a} = 0.3$ the ratio $\frac{m_o}{m} = 4.35$, while for $\bar{a} = 0.70$ the ratio is $\frac{m_o}{m} \approx 6.0$. For all configurations, mass removal at the rear zone of the models is insignificant. Comparison of the values of β and b from Table 1 reveals that the fundamental role in heat exchange during particle combustion in oxygen flow is that of diffusion resistance (Kritrin, FGiV, 1957) characterized by the term $1/\beta$.

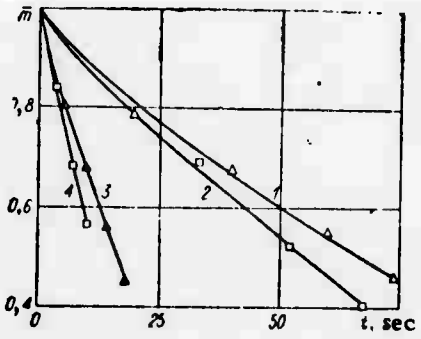

Fig. 2. Mass removal rate vs. time. Curve parameters are those of Fig. 1.

The mechanism of relative correspondence was therefore used to obtain very simple relationships which permit evaluation of the substance removal rate from the surface of a body in the stream of a chemically active gas in the presence of a heterogeneous chemical reaction. Mass removal rates from carbon particles of differing configuration were established from experimental data, and it was determined that the mass removal rate at the critical point and the surface change rate of a burning particle are constant. The temperature differential between the front and rear deges of the particle was also evaluated. It is shown that mass-removal data calculated by the method of correspondence are in satisfactory agreement with experimental data.

Rabinovich, L. B. and G. N. Sechenov.
Heat transfer conditions from a surface to a fluidized layer under pressure.
I-FZh, v. 22, no. 5, 1972, 789-794.

The effect of temperature, pressure, and gas composition on surface heat transfer to a contiguous fluidized layer was studied within the temperature interval 150 to 1000° C and at pressures from 0.5 to 30 atm. The test facility consisted of a device for investigating heat exchange in a fluidized layer, comprising an externally heated electric furnace, a tubular cooler, a carrier-gas heater, and control and measurement instrumentation. Two units were used: one for heating the wall temperature to 100 to 400° C at up to 50 atm; the other for heating from 400 to 1000° C, to the same pressure. The wall temperature of the external apparatus was maintained at a constant level in each series of experiments. In the initial mixture, gas was coupled with a pulverized catalyst, using particle sizes of 0.40 - 1.0 mm.

Used as the fluidizing gas composition were an equal mixture of nitrogen and CO_2, and two mixtures of nitrogen, H_2 and CO_2: (a) CO_2 16%, N_2 55%, H_2 29%, and (b) CO_2 25-30%, N_2 35%, H_2 35-40%.

As the pressure was increased from 0 to 30 atm (i.e., with increasing gas flow G, kg/h) within the 120 to 260° C range, and other conditions being equal, the heat-exchange coefficient α increased, despite a decrease of the gas linear velocity. The maximum value of α was not attained in the investigated range of pressures and temperatures, since the experiments were conducted at relatively low gas-stream velocities within the ascending curve of $\alpha = f(G, P)$ where P = internal pressure.

The value of α is definitely affected by the gas physical properties. Experimental results show that the greater the H_2 content the higher is the α, particularly with regard to the process of methane vapor conversion; α rises with increased temperature. With a mean temperature rise in the layer from 300 to 900° C, the absolute value of α_{tot} increases by a factor of 2.4-2.7. The relationship of the rise of α with increased pressure is valid at each temperature layer. At temperatures above 300° C, the increase of the difference between the apparatus surface temperature and the mean layer temperature becomes more pronounced. Data obtained during investigation of the surface heat transfer to a fluidized layer, with nitrogen as the carrier gas, were generalized by the relationship Nu = f(Re). An equation for calculation of the total (convective and radiative) heat transfer coefficient was derived on the basis of the experimental data:

$$Nu = 42.17\, Re^{0.9} T_{layer}/250,$$

where T_{layer} is the mean temperature of the fluidized layer; 250° C is the lowest value of T_{layer} adopted in the calculation of α.

Chernyshevich, I. V., and I. P. Zhuk. Three-dimensional problems of non-stationary thermal conductivity of solids under thermal destruction. IAN B, no. 2, 1972, 101-106.

A solution is presented to a boundary-value problem for heat conduction in solids with boundaries moving in accordance with an arbitrary law. The problem arises in surface breakdown by intense heat flux and gas ablation, and is related to the protection of structures and

assemblies against such intense heat by coatings undergoing phase transformations. Model configurations were a solid and a hollow cylinder, and a finite parallelepiped. In each case, the problem is formulated by a partial differential equation for heat conduction with initial and boundary conditions assuming that the total geometric surface area burn off. In the simplest case, of a solid cylinder with only one moving boundary, the heat conduction equation is

$$a\left(\frac{\partial^2 t}{\partial r^2}+\frac{1}{r}\frac{\partial t}{\partial r}+\frac{1}{r^2}\frac{\partial^2 t}{\partial \varphi^2}+\frac{\partial^2 t}{\partial z^2}-bt\right)+f(r,\ z,\ \varphi,\ \tau)=\frac{\partial t}{\partial \tau}, \tag{1}$$

and the initial and boundary conditions are

$$t[r,\ \mu(\tau),\ \tau,\ \varphi]=M(r,\ \varphi,\ \tau) \tag{2}$$

$$t[r,\ \eta(\tau),\ \tau,\ \varphi]=N(r,\ \varphi,\ \tau), \tag{3}$$

$$t[S(\tau),\ z,\ \tau,\ \varphi]=T_0(z,\ \varphi,\ \tau), \tag{4}$$

$$t(r,\ z,\ \varphi,\ 0)=f_0(r,\ z,\ \varphi). \tag{5}$$

For the hollow cylinder and the parallelepiped additional boundary conditions of the third kind are formulated, for the second and third boundary respectively. Equation (1) with conditions of (2) - (5) is solved by successively applying the Fourier cosine transform, Hankel transform, Green's function for the first boundary-value problem, and a contour integral. Application of the inversion formula to the finite integral transform yields the solution

$$t(r,\ z,\ \varphi,\ \tau)=\frac{1}{\pi S^2(\tau)}\left\{\sum_{k=1}^{\infty}\frac{\bar{\bar{t}}^*(\alpha_k,\ z,\ 0,\ \tau)J_0(\alpha_k r)}{J_1^2[\alpha_k S(\tau)]+J_0^2[\alpha_k S(\tau)]}+\right.$$

$$\left.+2\sum_{n=1}^{\infty}\sum_{k=1}^{\infty}\frac{\bar{\bar{t}}^*(\alpha_k,\ z,\ n,\ \tau)\,J_n(\alpha_k r)\cos n\varphi}{J_n^{12}[\alpha_k S(\tau)]+\left[1-\frac{n^2}{\alpha_k^2 S^2(\tau)}\right]J_n^2[\alpha_k S(\tau)]}\right\} \tag{6}$$

A similar procedure gives the final solutions of the problem for a hollow cylinder:

$$t(r, z, \varphi, \tau) = \frac{1}{\pi}\sum_{k=1}^{\infty} t^*(\alpha_k, z, 0, \tau)\, V_0(\alpha_k r)\} \{S_2^2(\tau)\{V_1^2[\alpha_k S_2(\tau)] + V_0^2[\alpha_k S_2(\tau)]\} - S_1^2(\tau)\{V_1^2[\alpha_k S_1(\tau)] + V_0^2[\alpha_k S_1(\tau)]\}^{-1} + \frac{2}{\pi}\sum_{k=1}^{\infty}\sum_{n=1}^{\infty} t^*(\alpha_k, z, n, \tau)\, V_n(\alpha_k r)\cos n\varphi \times \left\{S_2^2(\tau)\left[V_n'^2(\alpha_k S_2(\tau)) + \left(1 - \frac{n^2}{\alpha_k^2 S_2^2(\tau)}\right)V_n^2(\alpha_k S_2(\tau))\right] - S_1^2(\tau)\left[V_n'^2(\alpha_k S_1(\tau)) + \left(1 - \frac{n^2}{\alpha_k^2 S_1^2(\tau)}\right)V_n^2(\alpha_k S_1(\tau))\right]\right\}^{-1} \tag{7}$$

and a finite parallelepiped:

$$t(x, y, z, \tau) = \frac{8}{S_1(\tau)\, S_2(\tau)\, S_3(\tau)} \times \sum_{k=1}^{\infty}\sum_{m=1}^{\infty}\sum_{n=1}^{\infty} t(\mu_k, \eta_m, \gamma_n, \tau)\, W_1(\mu_k x)\, W_2(\eta_m y)\, W_3(\gamma_n z). \tag{8}$$

It is noted that to determine the temperature distribution for a hollow cylinder or a parallelepiped, it is necessary to: (a) find the roots α_k of a transcendental equation, such as

$$Y_n[\alpha S_1(\tau)]\, J_n[\alpha S_2(\tau)] = J_n[\alpha S_1(\tau)]\, Y_n[\alpha S_2(\tau)]. \tag{9}$$

for a hollow cylinder; (b) determine the kernel V_n of the integral transform, e.g.,

$$V_n(\alpha_k r) = Y_n[\alpha_k S_1(\tau)] J_n(\alpha_k r) - J_n[\alpha_k S_1(\tau)]\, Y_n(\alpha_k r), \tag{10}$$

and (c) apply the (7) or (8) formula. The laws of motion $S(\tau)$, $S_1(\tau)$, $S_2(\tau)$, and $S_3(\tau)$ of the boundaries in (4), and (6) to (10) are equicontinuous functions which do not vanish for any $\tau > 0$.

The solution is applicable to a variety of physical problems which can be described by parabolic equations with movable boundaries. Extension of the solution to more complex bodies (an ellipsoid, a paraboloid, and a hyperboloid) is planned.

Georg, E. B., Yu. K. Rulev, G. F. Sipachev, and M. I. Yakushin. Experimental study of ablation boundary layer in specimens under simultaneous action of convective and radiative heat fluxes. MZhiG, no. 2, 1972, 25-29.

The ablation boundary layer in asbestos-reinforced plastic cylindrical specimens with a spherically blunted nose was studied in an air plasma jet produced by a high-frequency electrodeless discharge. The discharge generated a 37 mm diameter plasma jet at 1 kg/cm^2 pressure with Reynolds number of 100 and a 30 m/sec velocity. The plasma, boundary layer, and specimen emission spectra were recorded simultaneously on a photographic plate by means of an optical system including an ISP-51 prismatic spectrograph. Plasma jet interaction with the studied material was recorded by motion picture camera at a speed of one frame/second. A sharp boundary was detected between the specimen and the boundary layer. The visible emission spectrum of the latter exhibited characteristic lines of the elementary constituents of the original material. The boundary layer emission intensity in the 3838-6483Å spectral range was comparable to or higher than that of the plasma. The temperature profile across the boundary layer (Fig. 1) was determined near the

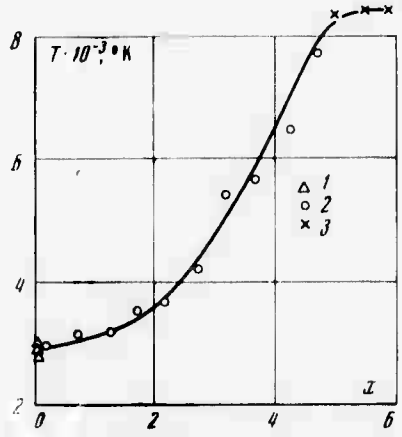

Fig. 1. Temperature of ablation surface (1), temperature profile across the boundary layer (2), and plasma temperature (3).

critical point from the spectral measurements (CN lines) of vibrational temperature of vapors in the boundary layer. The measurement accuracy was ±400°K. The spectroscopically measured plasma temperature was 8,500 ± 150°K and the true temperature of the ablation surface was 2,600 ± 200°K, where the latter was determined from measurements of the surface brightness. Temperature profile and IR motion pictures indicate that the boundary layer is separated from the specimen surface. According to the proposed model of the ablation boundary layer, gas formed by thermal destruction of the specimen is injected through the gas-body interface normal to the body surface. The convection component of heat flux is evaluated on the basis of this model. It was concluded that a decrease in convection by injection of the gaseous ablation products into the boundary layer is the principal mechanism of heat absorption.

Lutkov, A. I., B. K. Zymov, and V. I. Volga. The relationship between thermal and electrical conductivities of graphite. I-FZh, V. 22, no. 5, 1972, 932. (Annotation).

An attempt to correlate thermal conductivity λ with electric resistivity δ of graphite at high temperatures is described. Many researchers previously noted that the $\lambda \times \delta$ product is constant to a certain degree, but only at room temperature.

Experimental λ and δ data in the range 80 - 2,500°K range are given and the $(\lambda \times \delta)$ values are calculated for artificial graphites with 1.0 - 2.26 g/cm^3 specific weights. At a low temperature, the $(\lambda \times \delta)$ of individual graphites varied significantly. At room temperature, $(\lambda \times \delta)$ was nearly the same for the graphites studied. At T > 1,500°K, $(\lambda \times \delta) = 0.34 - 0.38$ V^2/degree and is independent of temperature for all graphites studied with the exception of those with lowest (1.0 g/cm^3) and highest (2.26 g/cm^3) specific weights.

Voronin, V. I., and A. Ye. Blazhkov. Thermal boundary layer on a noniso-thermal plate. IVUZ Aviatsionnaya tekhnika, no. 1, 1972, 119-123.

The equation of energy of a compressible laminar boundary layer on a semi-finite plate with different local boundary conditions is analyzed. It is assumed that the $0 \leq \xi \leq 1$ area of the leading edge, where $\xi = \xi / \ell$ and ξ is the longitudinal coordinate, is cooled to a constant temperature T_{wo}, and its equation of energy is solved by the known Crocco integral. Using this integral and a

Laplace transform, the equation of energy of the heat insulated section $1 \leq \xi \leq \infty$ of the plate is approximated with a relatively small error by

$$t(1-t)\frac{d^2i^*}{dt^2} + \frac{2}{3}(1-t)\frac{di^*}{dt} - pi^* = -p(a + b\sqrt[3]{t}). \qquad (1)$$

where the variable $t = u^{-3}$, p is the Laplace variable, a and b are the constants in the Crocco integral i, and * denotes the function in the transform space. In general form the (1) approximation, which also describes the boundary layer in the $1 \leq \xi \leq \infty$ section, is solved for i^*

$$i^* = AF(\alpha, \beta, \gamma; t) + Bt^{1-\gamma}F(\alpha_1, \beta_1, \gamma_1; t) + a + i_2^*. \qquad (2)$$

where $F(\alpha, \beta, \gamma, t)$ and $F(\alpha_1, \beta_1, \gamma_1, t)$ are hypergeometric functions, i_2^* is the particular solution of (1), A and B are the constants of integration, which are determined from the boundary conditions. Thus, $B = 0$ and A is expressed in terms of the hypergeometric functions and the logarithmic derivative of the Euler gamma-function Γ. Using (2), the temperature T_w of the heat-insulated surface of the plate is expressed through the Γ functions

$$\frac{T_w - T_{w0}}{T_0 - T_{w0}} = 1 - \frac{1}{9\Gamma^2(2/3)}\sum_{n=1}^{\infty}\frac{6n-1}{(n!)^2}\Gamma^2\left(\frac{3n-1}{3}\right)\frac{1}{\bar{\xi}^{\frac{(6n-1)^2-1}{36}}}. \qquad (3)$$

This method of T_w determination on a plate with a cooled nose is extended to the case of a surface with heat exchange. The method is illustrated by the example shown in Fig. 1.

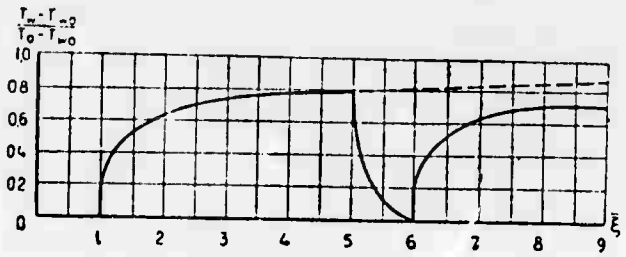

Fig. 1. Temperature distribution along a plate with cooling of the $5 < \xi < 6$ area according to the formula $q_w = 2(T_0 - T_{wo})$.

Fateyeva, N. S., and L. F. Vereshchagin. Melting curve of molybdenum up to 90 kbar. ZhETF P, v. 14, no. 4, 1971, 233-235.

A test is briefly described in which the melting curve of pure Mo under high pressure was measured by an optical method described earlier by the authors. The method is based on simultaneous determination of the radiation intensity ratios I_1/I_2 and I_2/I_3 of two pairs of narrow spectral regions, and their subsequent comparison with Planck's law. The experimental T(P) plots of Fig. 1 can be presented by the linear equation

$$T_M = 2883 + 0{,}8 \cdot 10^{-3} P \qquad (1)$$

where T is melting point in ^{o}K and P is the pressure in bars. The probable error is $\pm$% for both T and P measurements. A similar experiment was reported by Fatayeva et al on melting characteristics of graphite under high pressure [Explosion Effects Report No. 2, p. 58].

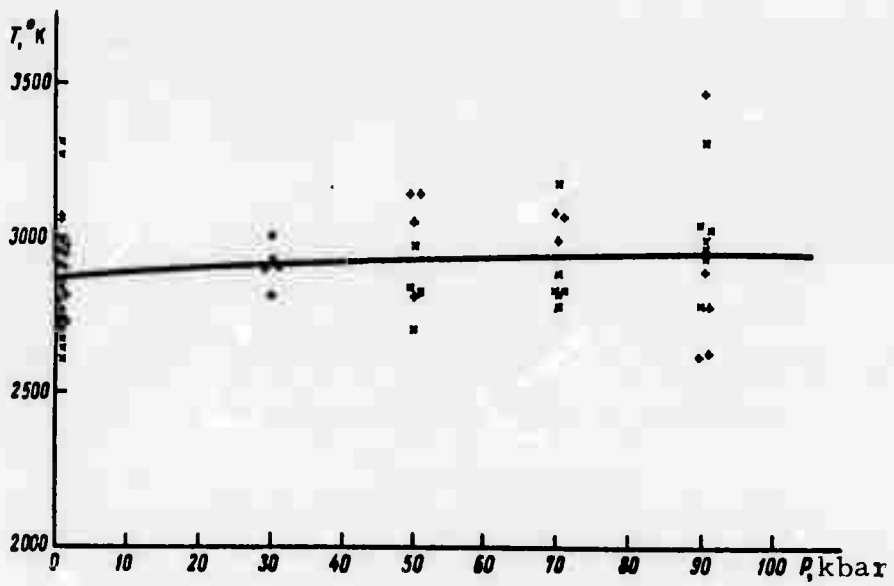

Fig. 1. Melting curve of Mo up to 90 kbar, calculated from all experimental points.
+ - temperature data of I_1/I_2 measurements,
x - temperature data of I_2/I_3 measurements.

Borovoy, V. Ya., Kharchenko, V. I. Experimental investigation of flow and heat exchange in the separation zone on an axisymmetric body with a conic shield. MZhiG, no. 3, 1972, 35-40.

The results are presented of an experimental investigation of the distribution of pressure and heat exchange on the surface of a conic shield mounted on a cylinder with a conic nose. The shield inclination angle was varied from 10 to 60°, the ratio of the cylinder length to the shield base diameter was $l/D = 0.5--2$. The experiments were conducted at Mach number $M_{\infty} = 5$, pressure $p_o = 8$ bar, stagnation temperature $T_o = 400--773^{\circ}$ K, and a Reynolds number, calculated on the basis of the total length model, $Re = 0.6 \times 10^6$.

Shadow photographs show that on a model with an angle of shield inclination $\varphi = 30^{\circ}$ and an angle of attack $\alpha = 0$, a separation zone develops, with shock wave formation at points of separation and attachment. At values of $\varphi \geq 30^{\circ}$, the laminar mixing layer in the stall zone becomes turbulent, and separation lines are clearly detected on the basis of points applied by washable paint. On a model with $\varphi = 30$ at $\alpha = 10^{\circ}$, points applied in the separation zone were practically not washed out at all.

Measurement of change of the angle of inclination of the stall zone to the cylinder generatrix, θ, in relation to the cylinder length at $\alpha = 0$ ($\varphi = 10, 20, 30^{\circ}$), revealed that with sufficient cylinder length, equal values of angle θ ($4--4.5^{\circ}$) were yielded for all shields; this corresponds to a separation point along the

cylinder beyond the inflection point, i.e., to free interaction. As the angle of attack is increased, the length of the stall zone on the windward side decreases sharply, and increases on the lee side. After the separation point moves along the windward side beyond the inflection point, the separation angle θ does not change with fur ther increases of the angle of attack and comprises 3.5°, i.e., differs little from the separation angle during free interaction at $\alpha = 0$.

Pressure was measured on the shield only. The pressure distribution along the relative length of the shield generatrix at $\varphi = 30^{\circ}$ was obtained for $\alpha = 0$, 10, and 30°. At $\alpha = 0$, the pressure in the separation zone is almost constant. Calculated values of the pressure coefficient C_p for the "fluid cone" formed by the stall zone agree with the measurement results. In the region of boundary layer, the pressure increases, and toward the end of the shield becomes constant. Analogous data were also obtained for tests of shields with other values of φ. The pressure on the windward generatrix increases when the angle of attack is increased and decreases on the lee generatrix. Experimental data for the region of attached flow on the windward generatrix at $\alpha = 10^{\circ}$ also coincide with the calculated values. In tests on models with $\varphi = 20^{\circ}$ and 30° at $\alpha = 30^{\circ}$, a pressure peak appeared on the windward generatrix as a consequence of interaction of the forward shock and the shock starting at the point of transition from the cylinder to the shield. At smaller angles of attack the region of interaction was located behind the shield. For heat tests the $\sim$ 0.5 mm thick shields were made of stainless steel. The specific heat flux was calculated in terms of the Stanton number, St.

The heat flux distribution along the length of the shield for $\alpha = 0$ has a maximum when $\varphi < 60^\circ$. When $\varphi = 20$ and 30°, the heat-flux maximum is behind the point of attachment, and at $\varphi = 45^\circ$ the two points practically coincide. At $\varphi = 60^\circ$ attachment takes place at the rear edge of the shield, and the maximal heat flux could not be measured. The value of the maximum Stanton number St* rises sharply with an increase of φ, primarily due to a gas-density increase and an angle of incidence increase of the stall-zone flow line with the shield generatrix. On the basis of the maximal value of the Stanton number St_o^*, computed on the basis of the flow parameters at the outer boundary of the stall zone, it is shown that during turbulent flow in the stall zone at $\alpha = 0$, the value $St_o^*/\sin(\varphi - \theta)$ changes relatively little in relation to φ. The values of St for various cylinder and nose-cone variants did not vary by more than 30%.

In a study of the influence of α on heat exchange, it was found that even at $\alpha = 1\text{--}2^\circ$, the heat flux distribution on the shield is considerably deformed due to stall zone deformation: on the windward generatrix the maximum is shifted forward, and on the lee side it is shifted to the rear, with the value of the maximal heat flux undergoing virtually no change. As α is increased to values ranging up to 30°, the degree of nonuniformity of heat flux distribution along the length of the generatrix does not increase; in many cases it even decreases considerably. This is because the separation zone length on the windward surface decreases and practically the entire shield is situated in an attached flow as α is increased.

VII. ATMOSPHERIC PHYSICS

Benediktov, Ye. A., G. V. Bukin, Yu. V. Kushnevskiy, S. N. Matyugin, N. P. Mozerov, Yu. K. Perekhvatov, and M. D. Fligel'. Reception of Kosmos-381 signals from a conjugate point region. Kosmicheskiye issledovaniye, no. 2, 1972, 302-303.

An attempt is described to detect satellite r-f signals from a conjugate point, with the object of precluding the possible anomalous magnetospheric or ionospheric modes that may be excited from ground-based transmitters in conjugate point experiments. The tests were done in December, 1970 using the Kosmos-381 satellite which broadcast at 2, 3.2, 5.6, 8.6, 10.4 and 12.8 MHz. Pulse power was 100w, and pulse width was 150μs at a 48 Hz repetition rate; reception was monitored with wideband delta or rhombic arrays at both the Moscow and Gor'kiy tracking stations. During part of the test period the orbital plane included both the receiver and conjugate points; the remaining orbits included the conjugate point only.

In the 13th recording session with transmission at 12.8 MHz, a signal from the conjugate point (lat. 39.5° S, long. 55° E) was clearly received at Moscow for an interval of 20 seconds, corresponding to a satellite travel of 150 km. The magnetosphere channel width was however somewhat less than this value, since the satellite path was presumably at some inclination to it, and also because the channel tends to "trap" the transmitted signal near its boundaries. Analogous reception at Gor'kiy was only for 0.25 to 0.5 sec, evidently because the satellite only grazed the waveguide channel. In some cases conjugate point reception was obscured by noise in the 12.8 MHz range; however there were cases where clear line-of-sight signals were recorded with no corresponding conjugate point reception.

Since the tests were conducted at various times of day and orbital inclinations, the authors point out that their data indicate the spatial and time variation in the magnetosphere channel.

Benediktov, Ye. A., L. V. Grishkevich, and V. I. Ivanov. Simultaneous measurement of electron concentration and collision frequency in the ionospheric D-region, using a partial reflections method. IVUZ Radiofiz, no. 5, 1972, 695-702.

In a related earlier work the authors described initial results in measuring electron density N in the D-layer by obtaining the correlation coefficient between backscatter of the ordinary and extraordinary wave components (IVUZ Radiofiz, no. 9, 1971, 1452). In that paper the feasibility of simultaneously determining the collision frequency ν_m from the same data was postulated; in the present article this is verified theoretically and experimentally. The analysis assumes a rectangular transmitted pulse τ at frequency ω and a sufficiently directional beam so that, neglecting absorption in the scattering medium, the correlation coefficient for both wave components may be found from

$$\rho_{A_0 A_x} = \frac{\sin^2 X}{X^2}, \qquad (1)$$

where $X = kL(\mu_0 - \mu_x)$; μ_0 and μ_x are refractive indices of the ordinary and extraordinary components; $L = c\tau/2$; and $k = \omega/c$.

Graphical results of ρ (N) are presented for an assumed set of ν_m, based on Eq. (1), and calculated for transmitted frequencies of 3 and 5.75 MHz. It is shown that with the assumed simplifications

the error in calculated N should not exceed 15 to 25% for $0.1 < \rho < 0.95$. Using the same model the authors arrive at theoretical values of $\nu_m(h)$ which are claimed to be accurate within 15--30%.

Test data confirming the foregoing were obtained in 1969-70 from vertical probes at 5.75 MHz and $\tau = 50\mu s$, with a $12^o \times 12^o$ directional pattern at medium latitudes. Further extensive tests were made at Gor'kiy in 1970 and are to be treated in a subsequent paper.

Mironov, V. L., and S. S. Khmelevtsov. Laser beam divergence during propagation in a turbulent atmosphere along an oblique path. IVUZ Radiofiz, no. 5, 1972, 743-750.

The authors develop expressions which define the turbulence broadening effect on laser propagation in the atmosphere. The general case of an inclined path is treated, requiring that different turbulence characteristics of specific altitude ranges be taken into account. The argument is given in terms of the function $C_n^2(x')$ which is defined as the structural characteristic of refractive index variation over a path length x'. Since this variation has been found to be a function of extended convection, it is convenient to examine C_n^2 directly as a function of altitude h, after the manner proposed by Tatarskiy. Thus for the dynamic boundary layer ($h < 50$ m) this characteristic is given by

$$C_n^2(h) = C_n^2(h_0)(h/h_0)^{-2/3}, \quad (1)$$

where h_o is some arbitrary transmitter height. At higher altitudes where free convection applies ($h \cong 1$ to 3 km), the relation alters to

$$C_n^2(h) = C_n^2(h_0')(h/h_0')^{-4/3}, \quad (2)$$

where $h_o' = 50$ m. For $h > 3$ km, it becomes

$$C_n^2(h) = C_n^2(h_0')\,(h/h_0')^{4/3} \exp\left(\frac{h_0 - h}{h_0''}\right), \qquad (3)$$

where $h_o'' = 10$ km, the thickness of the optically active atmospheric layer.

Using the foregoing expressions for C_n^2 (h) in a dimensionless fashion, the authors compare their calculated results with those of several other authors for altitudes up to about 10 km; those results are given graphically. A further analysis shows that less turbulence broadening is suffered when transmitting downward than upward through the atmosphere; this however is not contradictory if the finite dimensions of the transmitter aperture are considered, rather than the point source assumed in the theoretical calculations. It is also shown that for downward propagation, the maximum turbulence scattering will consistently occur at the same transmitter altitude; the authors' data put this at approximately 2 km.

Tsaplin, V. S. and L. V. Zubareva. Transient and spatial intensity distribution of excess radiation in the vicinity of the equator. GiA, no. 3, 1972, 536-537.

Satellites of the Kosmos series were launched from July 1965 through March 1969, into orbits with apogees of about 350 km, perigees of abo 200 km, and a 65° inclination to the equatorial plane, i.e. such that over 80% of the time the satellites were well below the radiation belts of the earth. A gasdischarge counter installed on each spacecraft registered on the basis of a direct passage, electrons with an energy of $E_e > 8$ Mev and protons with an energy of $E_p \gtrsim 60$ Mev. The

intensity of the recorded radiation in the vicinity of the equator was ~ 0.6 particles $cm^{-2} sec^{-1}$, which exceeds a previously recorded count of the primary cosmic-ray component in this region by an order of magnitude.

The stability of the intensity of this excess radiation corresponds to the stability of primary cosmic radiation. On this basis a curve was constructed of the intensity minima of excess radiation in terms of geographic coordinates (Fig. 1).

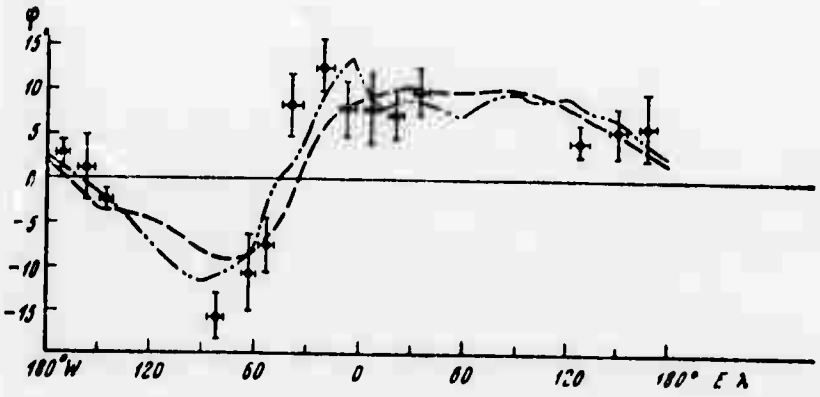

Fig. 1. Intensity minima of excess radiation.

The experimental values obtained by this method coincide well with the position of the cosmic-ray equator calculated by Kellog and Schwartz in an octupole approximation (point-dash line) and by Quenby and Webber with account taken of the nondipole part of the geomagnetic field (dashes). This suggests that the excess radiation is a secondary component, generated by cosmic-ray particles in the Earth's atmosphere and the housing of the unit. A relatively large mean-square error value is apparently explained by the statistical relationship of the secondary component multiplicity to the primary particle energy, and the influence of the Earth's magnetic field on the trajectory of the excess-radiation particles.

Katasev, L. A. and V. F. Chepura.
Investigation of movement of artificially ionized clouds in the upper atmosphere.
GiA, no. 3, 1972, 473-476.

Results are presented of simultaneous observations of the movement of artifical ionized and noctilucent clouds in the ionosphere. Measurements were made of 1) the velocity of ionized clouds on the basis of the Doppler effect reflected signals and 2) wind-velocity values, obtained in the same experiments using artificial noctilucent clouds.

The phase change of signals reflected from the ionized clouds was studied by two laser DME units operating at f = 24 MHz, which recorded the Doppler signal shifts on photographic film. Noctilucent clouds were photographed at two points by two aerial cameras. Ionized and noctilucent clouds were simultaneously formed by ejecting atomic cesium and sodium from a single container. Points for observation of the ionized clouds were situated virtually along the line of projection to the Earth of the point of cloud formation so that the Doppler-frequency phase shift of signals reflected from the clouds determined primarily by the movement of the clouds would differ little from one another at the observation points. A large difference of Doppler frequencies at the observation points during the experiment and, consequently, of cloud velocities, would testify to an essential influence of the space-time instability of the cloud structure on the phase change of the signals reflected from the cloud.

Two experiments were conducted over Volgograd in 1969. Ionized and noctilucent clouds were created on October 14, at 0523 hours local time, at an altitude of 120 km, and on October 22, at 0533 h at an altitude of 116 km. In contrast to the results of Gallacher and Barnes

(J. Geophys. Res., v. 68, 1963, 2987), the radial velocity of the ionized cloud at observation points P1 and P2 remained relatively stable. A statistical analysis of the experimental data shows that scattering of the radial velocity values of the ionized clouds at each observation point is principally governed by a normal distribution law.

The comparative values of radial velocity of the ionized clouds and the mean-square deviations at both observation points differ little. Due to the relatively large distance between the observation points, no correlation was made of the instantaneous phase changes of the field of the wave reflected from the ionized cloud. It is concluded that the wave phase changes reflected from the cloud and averaged over 0.5-second observation intervals, are determined principally by the cloud movement. This is supported by a comparison of the values of the velocity of the noctilucent cloud (coinciding with the wind velocity and averaged for the time of each experiment) with those of the ionized cloud. In both experiments, the difference between the velocity of the ionized cloud and the wind velocity is within the limits of experimental error.

The results of the experiments show that the phase changes of a wave reflected from an ionized cloud, even when averaged at 0.5-second observation intervals, are determined primarily by the cloud movement. Phase methods can therefore be used for investigating the movement of ionized clouds in the upper layer of the atmosphere. The results of Gallacher and Barnes, referred to above, are apparently explained by an inadequacy of the method for measuring the signal Doppler phase shift as reflected from the ionized clouds.

Kon'kov, A. A. and A. V. Vorortsov. Experimental investigation of infrared radiation from nitrogen. OiS, v. 32, no. 4, 1972, 655-660.

Infrared radiation from the free-free transitions of electrons in fields of nitrogen atoms is discussed. The aim was to eliminate some contradictions in the data on the infrared radiation from nitrogen, and to expand the range of conditions for infrared radiation investigations.

Nitrogen absorption coefficients were measured in the temperature range of 7000-8500° K, at pressures of 30-75 atm, and wavelengths of 2-6 μ. The nitrogen was heated by a shock tube, and the nitrogen gas parameters were determined on the basis of the shock-wave velocity. It is shown that the absorption from the free-free transition of electrons in nitrogen atom fields can be described by the relationship obtained by Firsov and Chibisov (ZhETF, v. 39, 1960, 1770) if $\sigma'_N = 1.6 \times 10^{-15}$ cm^2, and $\sigma'_{N_2} = 2.7 \times 10^{-15}$ cm^2, where σ is the electron elastic scattering cross section.

Andreyev, Yu. P., Ye. V. Gusev, and I. A. Semiokhin. Equilibrium in nitrogen-oxygen mixtures at high temperatures. ZhFKh, v. 46, no. 6, 1430-1432.

Equilibrium in nitrogen-oxygen mixtures within the temperature range 298 to 20,000° K is considered to evaluate the processes occurring in these mixtures in a pulse-discharge plasma. The investigation deals with two mixture ratios: $N_2:O_2 = 1:1$ (equimolecular mixture), and $N_2:O_2 = 4:1$ (air). The equilibrium was calculated for pressures which permit the operation of xenon flashlamps in an admixture of nitrogen and oxygen (760 torr) or in pure mixtures of nitrogen and oxygen (50 torr).

Temperature relationships of the equilibrium concentrations (in terms of mole fractions) of nitrogen-oxygen plasma products within the indicated range were calculated for $N_2:O_2$ = 1:1, 760 torr; $N_2:O_2$ = 1:1, 50 torr; $N_2:O_2$ = 4:1, 760 torr; and $N_2:O_2$ = 4:1, 50 torr. Curves of N_2, O_2, NO, O, N^+, O^+, and e were plotted for the initial mixtures and pressures. The curves show that as the temperature increases, the equilibrium-concentration curves of NO, N, and O pass through a maximum. The position of the maxima on these curves is virtually independent of the mixture composition, but the maxima shift toward higher temperatures as the pressure rises. The absolute value of the equilibrium product-concentration maxima is also a function of pressure. The maximum value of the equilibrium concentration of NO consequently rises with pressure. At concentrations of about 10^{-2} mole fraction, O_2 molecules disappear at 5000-6000° K, NO at 6000-7000° K, N_2 at 8000-9000°K, N and O atoms at 18,000-20,000° K. The N^+ and O^+ ions appear at 8000-9000° K.

VIII. LASER SIMULATION AND RELATED EFFECTS

Askar'yan, G. A., and S. D. Manukyan. Acceleration of particles by a moving laser focus, focusing front, or ultrashort laser pulse front. ZhETF, v. 62, no. 6, 1972, 2156-2160.

An analysis is given of several ways in which the high field gradient in a laser pulse can be used to accelerate electrons or ions in a controlled fashion. If the mean force exerted on a particle in an e-m field of amplitude E_o (r) and frequency ω is expressed as

$$\mathbf{f} = -\frac{e^2}{2m\omega^2}\nabla(E^2)_{mean}$$

then it can be shown that, for example, a neodymium laser generating nanosecond pulses in the 30 Gw range will produce an effective field E_{eff} of approximately 1 Mv/cm, while a picosecond pulse of 3×10^3 Gw will yield 100 Mv/cm. Gradients of this magnitude when given a controlled lateral displacement (swept beam) or axial displacement (change in focal point or beam divergence) can in theory be used for selective particle acceleration. One method for doing this would be programmed refocusing of annular portions of the laser wavefront, using corresponding portions of a focusing lens; another would be a programmed refocusing of the beam along a selected path. In the latter case it is shown that a channel with reduced nonlinear absorption can be generated for charged particle motion. In the case of low coulomb attraction between electrons and ions, electrons would essentically be accelerated as if free; at sufficiently high coulomb forces an ion acceleration component would appear. In conclusion the authors suggest that the moving-focus technique could be extended to provide macroscopic particle acceleration.

Semenova, V. I. Electromagnetic wave reflection during oblique incidence on a moving ionization front. IVUZ Radiofiz, no. 5, 1972, 665-674.

An extensive theoretical analysis is given of the interaction of a monochromatic wave with a plasma boundary. The particular case considered is of inclined incidence of monochromatic TE and TM waves upon a sharply defined boundary of a plasma half-space, where the plasma is generated by ionizing radiation acting on a neutral gas. For simplicity the incident pulse is assumed arbitrarity narrow and the dielectric constant outside the plasma is taken to be unity. It is shown that when the E-field normal to plane of incidence, the solution for the inclined incidence case is essentially the same as for normal incidence. With the TM wave, however, inclined incidence is shown to generate two axial waves in addition to the transverse ones, at any given frequency of the incident wave. Formulas for the reflection and transmission of the latter are obtained and analyzed in terms of the idealized plasma parameters.

Kuznetsov, A. Ya., I. S. Varnasheva, A. A. Poplavskiy, and G. P. Tikhomirov. Destruction of reflective dielectric coatings by laser radiation. OMP, no. 3, 1972, 39-42.

The resistance of reflective coatings to laser radiation was studied using zinc sulfide and magnesium fluoride coatings. The coatings were applied by thermal evaporation in a vacuum, and the reflection factor was $R = 90\%$ at $\lambda = 0.7\,\mu$. The flux falling upon the specimen was controlled

by glass filters at a constant radiation energy of a single-pulse multimode ruby laser, with ≈40 nsec a pulse duration. The purpose was to find the number of bursts the coating would endure at various energy-density values below the limit value, i.e., to find the threshold of destruction for multiple radiation effects. The reference threshold of destruction was the number of bursts n at which the mirror transmissibility increased by 30%. The energy density limit (threshold of destruction) at which the coating was destroyed with one burst was also measured. The reference density criterion in this case was the appearance of plasma, recorded photoelectrically or visually.

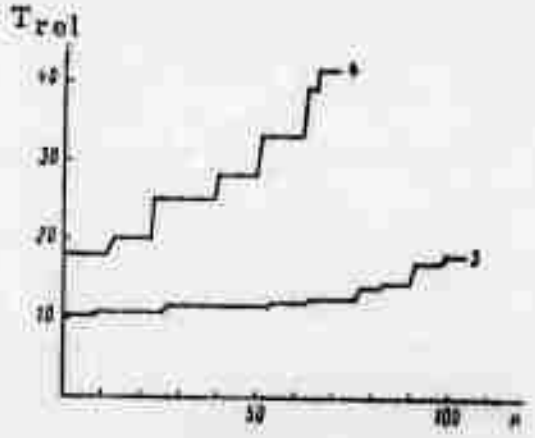

Fig. 1. Transmissibility variation in relative units for multiple radiation effects on two coatings.

Experimental relationships for the threshold energy density W, at which destruction begins at the n-th burst as a function of the number of exposures n, are presented in Fig. 2.

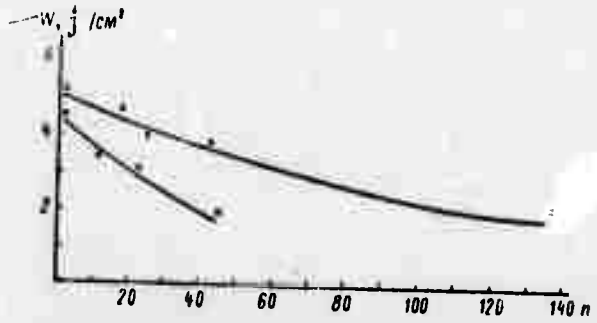

Fig. 2. Threshold characteristic, x- experimental values up to n = 140

The values in Fig. 2 are approximated by a function of the type

$$W_n = W_1 \times e^{-\beta(n-1)}$$

where W_1 is the threshold of destruction for one burst, W_n is the threshold of destruction for n bursts, and n is the number of bursts. The coefficient β for coatings produced by the same technique is 0.0080-0.0160. This ratio is an approximate one since it was determined for n = 140; however, it can be seen from (1) that the relationship of the destruction threshold to the number of bursts is cumulative. Although the coating properties for β were not determined, this value is always higher for coatings with a one-burst lower destruction threshold. Coating transmissibility increases substantially with a burst increase prior to the appearance of plasma (Fig. 1), although coating destruction is not observed visually. Electron-microscope observations show that, prior to the plasma appearance, the transmissibility increase is accompanied by microdestruction of the coating surface, which increases with the number of bursts. This form of destruction begins even before the change of coating transmissibility.

Assuming the destruction process is a thermal one at the absorption centers (microimperfections), a formula is presented for determining the index of absorption of the microimperfections, together with an example of its application.

Kantorovich, I. I. Frequency dependence of optical breakdown in gases. ZhPS, v. 16, no. 4, 1972, 605-610.

An analysis is given of the contribution of atomic excitation processes, particularly avalanche ionization, to optical breakdown in gas. The study is generally limited to the area around breakdown threshold, $\sim 10^6$ v/cm, with argon and xenon used as hypothetical media. Expressions are derived for the probability $f(\omega)$ of continuous ionization of Ar and Xe, and these results are plotted in Fig. 1.

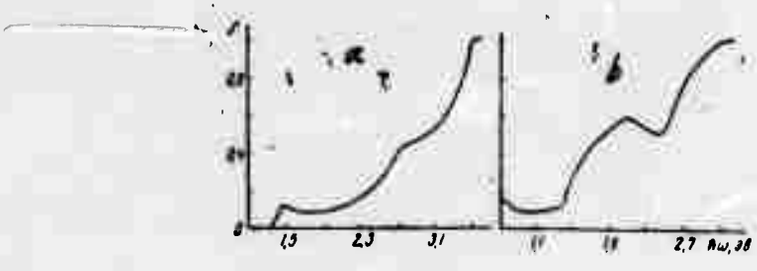

Fig. 1. Frequency dependence of ionization probability for Ar (a) and Xe (b). ω = optical frequency.

Breakdown threshold vs. beam frequency is shown in Fig. 2, which

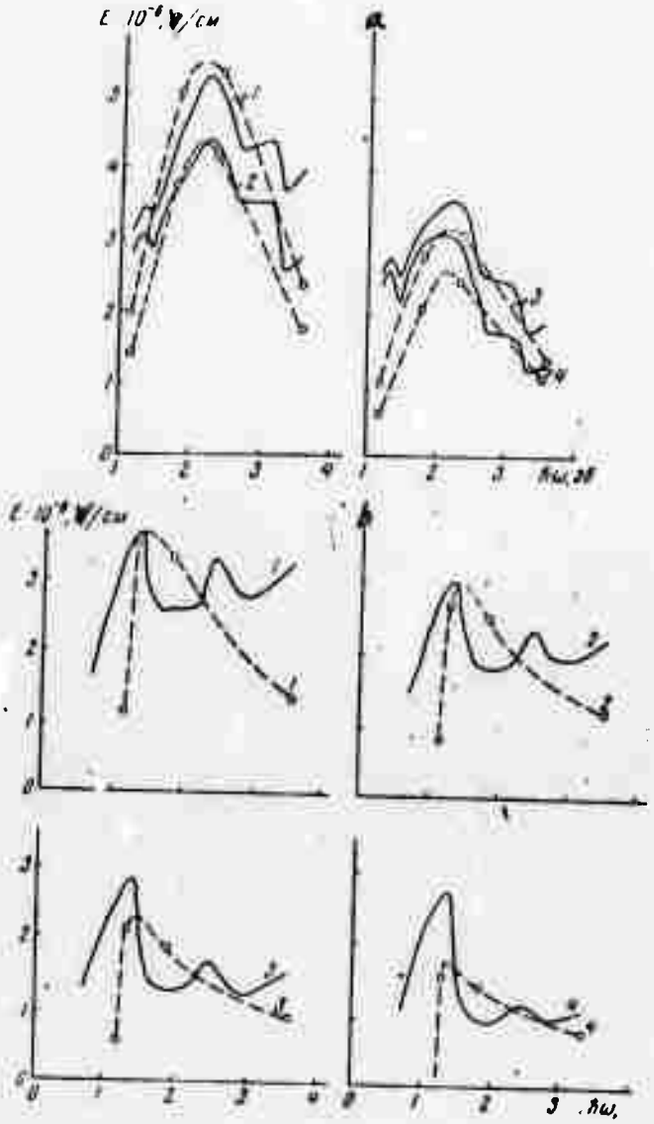

Fig. 2. Frequency dependence of breakdown threshold in Ar (a) and Xe (b) at pressures of 1000 (1); 2000 (2); 4000 (3) and 8000 torr (4). Solid line - theory; dashed - experiment.

compares theory with earlier experimental results. The divergence seen at lower frequencies and higher pressures is ascribed to increased multiphoton ionization probabilities owing to local nonuniformity.

Kuznetsov, A. Ye., A. A. Orlov, and P. I. Ulyakov. Pulsed regime for vaporizing optical materials by CO_2 laser radiation. IN: Sbornik. Kvantovaya elektronika, Moskva. no. 7, 1972, 57-60.

An analysis is given of experimental results on the interaction of CO_2 laser radiation (λ = 10.6μ; constant power density = (0.5-2) 10^4 w/cm^2) with a series of optical materials, as reported by Bubyakin et al (FIAN, 1969, 34p), where a shielding effect in the evaporation process of the substance and cavity formation were noted. Time characteristics of cavity depth l_k and the length of the luminous part of the flare l_f for KV quartz glass are plotted in Fig. 1. The evaporation displays a clearly

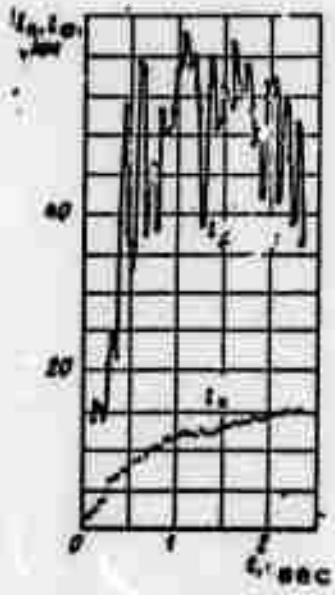

Fig. 1. Relationship of cavity depth l_k and flare length l_f to irradiation time for quartz glass ($q = 1.9 \times 10^{14}$/cm^2)

pulsating character with an irregular oscillating frequency of 5-10 Hz. Average deepening rates in the pulsating period and in steady-state evaporation are tabulated for various materials. This qualitative characteristic was observed in all experiments, with quartz as well as with other optical materials. The only variation was in the pulsation amplitude and the steady-state regime discharge time. Two main processes, namely gaseous phase dispersion and emission shielding lead to the pulsating nature of cavity formation. The pulsation damping of LK-5, K-8 and other glass types occurred more rapidly than with quartz glass. A steady self-adjusting evaporation regime was observed through to the complete piercing of a 60 mm thick quartz specimen, and with splitting of other materials. The pulsating nature of the process up to the self-adjusting regime is apparently common to all substances. The damage products of these substances also exhibit absorptivity at the active irradiation frequency. The authors conclude by giving a system of approximate equations for the dynamic low-temperature evaporation of dielectrics, taking vapor absorption into account.

Volosevich, P. P., and Ye. I. Levanov. On self-similar motions of a two-temperature plasma. IN: Sbornik. Teplo- i massoperenos, v. 8. Minsk, 1972, 29-35. (RZhMekh, 9/72, no. 9B119) (Translation)

A self-similar solution is analyzed to the problem of dispersion of an ionized gas in vacuum, occurring from a laser-target interaction. The case is considered for a powerful laser source interacting with a plane solid surface. The plasma is treated as a two-

temperature hydrodynamic approximation, taking into account the energy exchange between electrons and ions; electron thermal conductivity; and ion drag. The self-similar solution has the form of a temperature wave propagating through a given "noise" level at a finite velocity. Between the temperature wave front and the vacuum-target interface a shock wave occurs, at whose front the electron temperature is continuous while the hydrodynamic parameters and ion temperature undergo discontinuities. At the target face the ion component of temperature goes to zero, while the electron component has a non-zero value. Calculations show that there are two distinct modes of heat propagation, namely subsonic and supersonic.

Barmin, A. A., and A. G. Kulikovskiy. Boundary conditions at the surface of a discontinuity, occurring from the interaction of powerful radiation with metal. IN: Sbornik. Nauch. konf. In-t mekh, Mosk. universiteta, Moskva, May 22-24, 1972. Abstracts of papers. Moskva, 1972, 7. (RZhMekh, 9/72, no. 9B920) (Translation).

The structure is studied of the narrow transition zone which appears upon the interaction of powerful beamed radiation with metal, for the case in which the incident radiation is entirely absorbed. A complete system of boundary conditions is obtained for the surface discontinuity which is used to model the transition zone.

Nikiforov, Yu. N., V. A. Yanushkevich, and A. V. Sandulova. Change in electrical properties of p-Si crystal whiskers from the action of giant laser pulses. FiKhOM, no. 3, 1972, 132-134.

Laser-induced change in the resistivity ρ of p-Si whiskers is described. The whiskers were grown along the [111] axis, had a hexagonal cross section, and ranged in length from 3 to 7 mm. Specimens were exposed to 50 nsec giant pulses from a ruby laser, with the laser beam normal to the crystal axis. Impact densities were varied over several tens of joules/cm^2, up to the damage threshold which was in the range of 35 - 45 j/cm^2. The data are presented as resistivity variation $\Delta R/R_o$ in exposed specimens as functions of whisker geometry, ambient temperature and initial ρ. Typical results at an exposure of 22 j/cm^2 show a sharp rise in R by about 12-15%, followed by an exponential decay back to about the initial value, at a time constant $\cong$20 milliseconds. Of the possible mechanisms considered for the alteration effect (photoeffect, crystal heating, piezoeffect, defect formation) it is shown that point defect formation is the most probable factor. Defect levels, estimated to reach 10^{17}/cm^3, were effectively annealed out in all cases in 30 milliseconds or less.

Boyko, Yu. I., and A. K. Yemets. Study of laser self-focusing in alkali-halide single crystals, according to data on shift of the damage center. DAN, v. 206, no. 2, 1972, 319-322.

Experimental results are described of laser damage phenomena in KCL and KBr crystals, with the object of determining the

extent and effect of self-focusing in the crystal. A free-running Nd glass laser was used developing 100 μsec pulses to a maximum of 16 j. Target specimens were parallelepipeds 30x30x100 mm; the laser beam entered normal to an end face as shown in Fig. 1, using a lens with f = 55 mm.

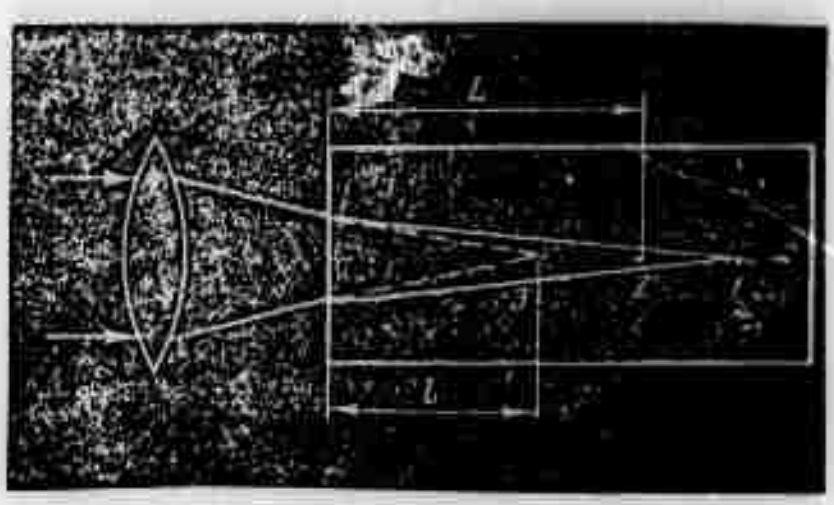

Fig. 1. Configuration for self-focusing experiment.

Results were analyzed in terms of the actual distance L of beam focus from the entrance face, and lens focal distance ℓ (Fig. 1). In the absence of nonlinear effects the approximate linear relation $L \cong n_o \ell$ should apply, where n_o = nominal refractive index; this proved to be the case for KCL, whereas for KBr the damage center was found to shift toward the laser source such that $L \sim \ell^2$. The effects are compared in Fig. 2, showing the

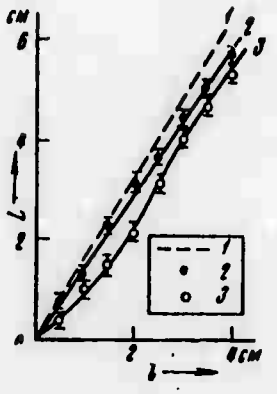

Fig. 2. Shift of damage center vs. lens focal distance
1 - calculated for KBr; 2 - KCl; 3 - KBr, actual

nonlinear self-focusing response of KBr. The latter effect suggests a thermal mechanism, which was confirmed by further tests on KBr specimens in a heat chamber in which $n_o(T)$ as well as $dn_o/dT(T)$ were measured. This showed that at 0.6 T_{fusion} and above, dn_o/dT takes on positive values which would account for the observed self-focusing in KBr.

Uglov, A. A., A. A. Zhukov, A. N. Kokora, M. A. Krishtal, and M. Kh. Shorshorov. "Shift" of critical points under laser heating of carbon-iron alloys. FiKhOM, no. 2, 1972, 3-8.

The "shift" of critical points in steel heated by a laser beam is analyzed. Allowance is made for nonuniform distribution of specific heat flux on the metal surface, and hence different volumetric heating rates. Under conditions of rapid heating and cooling rates, as in metal treatment by a laser beam, "shift" of critical points becomes important in micrographic determination of temperature within the metal after cutoff of the laser pulse. Using a theoretical formula, numerical data were obtained for heating rates $dt/d\tau$ in ShKh15 perlitic steel at various depths z and distances r from the center of a beam spot on the metal surface. Concentration coefficient $k = 80\ cm^{-2}$ was used in calculations of power density distribution on the surface. The calculated $dt/d\tau$ versus r plots (Fig. 1) show that, at $q_o = 0.92 \times 10^5\ w/cm^2$, $dt/d\tau =$

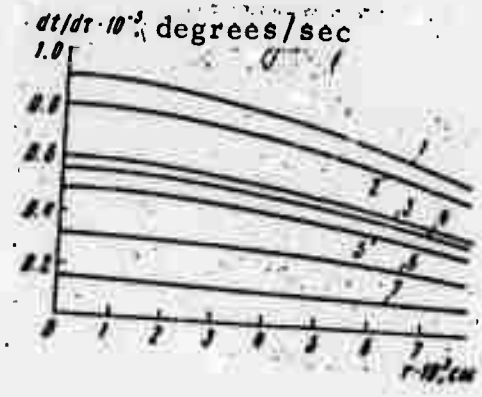

Fig. 1. Heating rate of ShKh15 steel by laser pulses of 0.5 millisec width versus r at z(cm) = 3.10^{-3} (1), 2.10^{-3} (2), 1.10^{-3} (3), 5.10^{-3} (4), 0 (5), 6.10^{-3} (6), and 7.10^{-3} (7).

10^5 degrees/sec, and that dt/dτ can vary by a factor of five in the region where temperature may exceed the perlite-to-austenite transformation point (A_1). At the cited dt/dτ , the shift t_x of point A_1 for ShKh15 steel was calculated to be ~ 200° C from

$$t_x = \left(\frac{k_1^2 x^2}{4D}\right)^{1/6} \cdot v^{1/6}$$

where k_1 = 110 degrees is the angular coefficient determined from the Fe-Fe_3C phase diagram; $\nu = 0.5 \times 10^5$ deg/sec is the heating rate in the critical temperature range, and $\bar{D}$ is the coefficient of carbon diffusion in austenite. The maximum Tx variation due to difference in v within the metal was 1.7. It was concluded that steel of a complex composition is not suitable for a study of temperature fields under conditions of a very rapid heating. In view of this conclusion, a micrographic study was made of type 45 and U8 hypoeutectoid carbon steels in a surface area casehardened by laser radiation. The micrographs show that the temperature range of A_1 transformation is enlarged up to the liquidus, and the A_3 transition point practically disappears with the ferrite lattice coexisting with melted austenite. A sample result of U8 steel exposure is shown in Fig. 2.

Fig. 2. Microstructure of type V8 steel with a perlite structure in the laser heating zone. A- fusion boundary; B- limit of thermally affected zone. (X 1300)

Goncharov, V. K., A. N. Loparev, and L. Ya. Min'ko. Self-igniting pulsed optical discharge in an erosive laser plasma. ZhETF, v. 62, no. 6, 1972, 2111-2114.

A variant on the optical plasmatron is described in which a self-igniting optical discharge is obtained from irradiation of a target surface. The technique was to defocus the incident beam such that the focal point was several millimeters above the target surface; vapor products from the surface, traveling at about 100 m/sec, would ignite on reaching the focal point and provide a "hanging" optical discharge for the remainder of the laser pulse. The experiment cited used an Nd glass laser at 1.5 μs pulsewidth and generating relatively low surface intensities on the order of $10^6 w/cm^2$. Various metals and dielectrics were tested as target materials, including ebonite, textolite, brass and a type POS-40 alloy. Depending on the material, a stable discharge was achieved in a 10 - 20 mm range above the target surface; spectral studies show discharge temperatures $\simeq 22,000^{\circ}K$. Streak photos of the discharge development are given; Fig. 1 shows one form of the discharge.

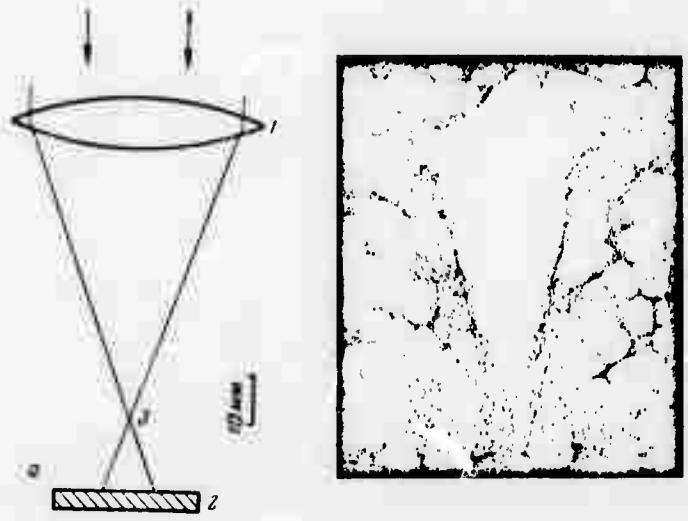

Fig. 1. "Hanging" optical discharge.

The authors suggest adapting the effect to a c-w discharge, using a CO_2 laser for excitation. The effect is claimed as the first of its kind obtained at atmospheric pressure.

Fanchenko, S. D., and G. V. Sholin. Possible mechanisms of turbulent heating of a plasma by ultrashort laser pulses. DAN SSSR, v. 204, no. 5, 1972, 1090-1093.

The authors consider the initial ionization phenomena arising from interaction of a picosecond laser pulse with a very dense plasma. A feature of this case is that the optical field strength E is comparable to intra-atomic field E_a; this results in an ionization time τ_{ion} on the order of or less than electron-atom on electron-ion collision time, and possibly less than the laser wave period. The model used assumes a picosecond pulse with optical

frequency Ω falling on a condensed neutral target. During the first portion of the optical wave rise time, light penetrates the target virtually without ionization taking place; as the optical field approaches its peak of E, ionization begins but with an electron plasma frequency $\omega_{p\ell}$ still below Ω. As $E \longrightarrow E_a$ the affected electrons proceed from bounded to unbounded motions in a time interval $\approx 10^{-16}$ sec. The authors then treat the two general intervals of collisionless plasma heating which ensue, namely when $\omega_{p\ell} < \Omega$ and $\omega_{p\ell} > \Omega$. Ionization parameters are obtained taking into account the magnetic piston effect exerted by the optical field when $\omega_{p\ell}$ overtakes Ω. Results show that at this point a beam of electrons forms in the focal region which may attain directional energies of 10^4 ev. Calculations based on a typical set of plasma parameters show that this current may exist for up to 10^{-12} sec. and reach densities above 10^{12} a/cm^2. It is emphasized that these deductions apply only to the initial one or two periods of laser pulse oscillation, applied to a neutral medium. Analogous effects from shock-wave and electron beam heating of a plasma are also noted.

Laboratory of laser beam mechanics. Nauka i zhizn', no. 2, 1972, 54-56.

Tests on mechanical effects of laser beams on optically transparent polymers are discussed. The destruction of plexiglass when exposed to a laser beam is explained by the presence of structural inhomogeneities. This was proven by experiments using a measured quantity of fine dust particles added to a polymer test specimen. After laser exposure, the maximum number of

damage centers was found to correlate with the number of injected microadmixtures. The polymer destruction process takes place in three stages: 1) generation of opaque centers; 2) heating and decomposition of material in the center region, and 3) destruction of the material surrounding the center. The cause of the thermal centers in polymers exposed to laser beams is not known, but it is assumed that thermal stress produces cracks in polymers, which strongly absorb radiation energy. Three photographs are given illustrating the destruction of a clear plastic by laser beam.

Laboratory of polymer mechanics. Nauka i zhizn', no. 2, 1972, 53-54.

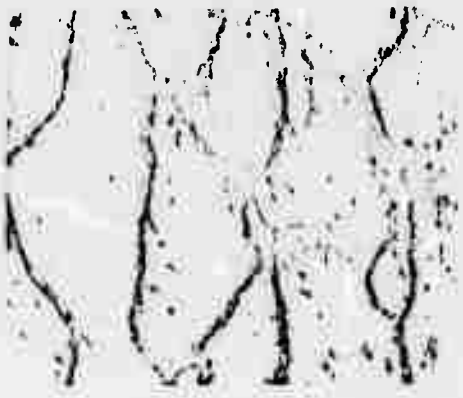

Fig. 1. Microstructure of plexiglass. Distinct boundaries divide the substance into separate aggregates of a size on the order of a micron.

Findings of investigations of the relationship between the strength and structural properties of polymers are briefly reviewed. Laser beam radiation caused destruction of polymers, usually along the boundaries of structural formations. The structural bond of a plexiglass was about 10 times weaker than

the molecular strength; accordingly, destruction was noted along the bonds well before molecular destruction. Molecular destruction can be caused by both heat and light. The wavelength of laser radiation is such that at low intensities unstressed polymer molecules do not absorb the waves; but internal destruction does take place and cracks are observed. The aggregate structure of the substance plays an important role; e. g. the less the aggregate size, the greater the amount of cracks in polymers. The investigations show that organic glass and other amorphous polymers contain hyper-molecular structures. Figure 1 shows the micro-structure of a plexiglass.

Geguzin, Ya. Ye., A. K. Yemets, and Yu. I. Boyko. Lowered optical strength of transparent solids with macroscopic defects. FTT, no. 5, 1972, 1565-1566.

An experiment is briefly described which attempted to correlate the degree of porosity in glass with its optical strength σ in laser applications. The case considered assumes that the characteristic linear dimension of the pore is greater than laser wavelength λ ; in such cases for glass or ionic crystals, as much as 70% of light incident on thepore may be reflected, resulting in interference with the transmitted beam and generation of thermal damage centers. Tests to show this effect were done with a silicate glass containing a dispersed powder, sintered to form a porous medium with pore size $\approx$ 5 microns and a mean pore spacing of 30 microns.

The porous glass was exposed to a He - Ne laser beam at 1.06 μ and a 50 msec pulse width, together with a non-porous glass. Results show that for the latter, σ was 6×10^{14} erg/cm^2· sec, dropping to 2.5×10^{14} erg/cm^2· sec for the porous specimen. The relation of the pore structure to color centers is noted as having a definitive effect on the optical strength characteristics. In another step of the test the porous medium was modelled on a larger scale by using spherical quartz glass beads, suspended in a medium with a higher refractive index than the beads. No other data are given for this portion; however, Fig. 1 shows the medium, and an interference pattern obtained also at $\lambda = 0.63\mu$. The results with the

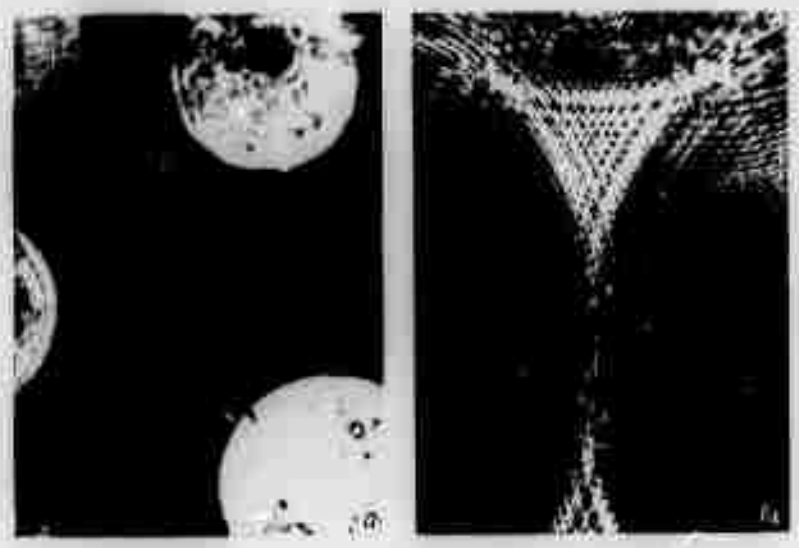

Fig. 1. "Pore" model, and interference pattern parallel to equatorial plane. X240.

model were effectively identical to those with the original sintered glass.

Batanov, V. A., V. K. Goncharov, and L. Ya. Min'ko. Powerful optical erosion plasmatron. ZhPS, v. 16, no. 5, 1972, 931-934.

A versatile laser-driven plasmatron is described which may be compared to the one described previously by Goncharov et al in this report. In the present design the simple chamber shown in Fig. 1 was used to

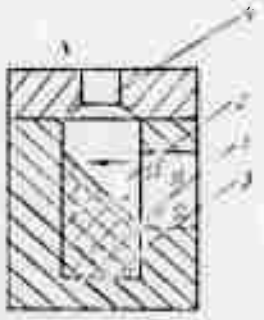

Fig. 1. Laser plasmatron
1- quartz window; 2- chamber;
3- target material; 4- exit nozzle

generate a plasma jet from any given target material, with the plasma driven out through the nozzle by generated pressure. By varying pulse parameters, chamber dimensions, fill gas, etc., a wide range of plasma jet characteristics can be obtained, ranging from subsonic to supersonic. The authors used an Nd glass laser at 0.8 millisecond pulses of 5 kj peak energy, in a quasi-cw regime, to develop target surface densities on the order of 10^6 w/cm^2. Glass textolite was used as target material, and helium at pressures from 5×10^{-2} ton to several atmospheres served as the fill gas. The many possible variations in jet parameters are discussed and both high-speed and streak photos are given of jet propagation. Table I compares results of two modes. The results generally show the versatility of this type of low temperature plasmatron.

Jet type	E, joules	Nozzle dia., cm	Chamber pressure, atm	Exit velocity km/sec	Adiab. index, γ	Mach no.
With shock wave	3.0	0.9	11	3.1	1.67	—
With periodic structure	2.2	0.9	8	2.6	1.67	1.9

Table I. Comparative data on supersonic nondivergent plasma jets

Aseyev, G. I., and M. L. Kats. Destruction mechanisms of alkali halide crystals and multi-photon ionization of impurity centers. FTT, no. 5, 1972, 1303-1307.

The destruction of a series of natural and impure alkali halide crystals (NaCl, KCl, KBr, NaBr, KCl-Eu, KCl-Ag, KCl-Tl, and KCl-In) under the effect of ruby and neodymium lasers was investigated in a free-running regime (energy = 1.5 joule, duration = 500μsec). Beam focusing on the specimens was done by f = 50 and 150 mm lenses. The destruction mechanism in crystals is explained in terms of Brillouin forced dispersion and local heating. The temperature at the damage site was approximately 5000°C at a near critical power density. Forced dispersion components were not observed. Results show little likelihood of destruction due to hypersonic phonons and high-frequency breakdown; the primary destruction mechanism is rather the local heating associated with absorption of a portion of the laser energy by crystal structure defects. The dynamics of the destruction process and causes of optical fatigue in alkali halide crys-

tals are outlined. It is shown that a decrease of at least one unit of the suggested photon level of the multi-quantum excitation process in photoconductivity of activated alkali halide crystals is associated with the thermal ionization of excited states of impurity centers. Graphical and photographic data of experimental results are included.

Bedilov, M. R., K. Khaydarov, and Kh. Babadzhanova. Nature of radiation defects formed on the surfaces of solids by ruby laser radiation. IAN UzbSSR, Ser. fiz-mat. nauk, no. 2, 1972, 66-68.

Results are described of an experimental investigation of damage processes on the surface of solids from ruby laser radiation in a free-running regime. Radiation energy was 1-3 joules and maximum power density was $\sim 10^7$ watt/cm^2; the beam was focused using a f = 50 mm lens. Targets were W, Mo, Ni, Zn, and Si, purified by laser radiation and placed in a 10^{-6} torr vacuum. Radiation processes were studied using microscopic and oscillographic methods, which provided data on integral and time characteristics of target surface defects during the laser pulse period. Integral defects formed by 800 μsec exposure were studied by microscope. In the 0.6-2 joules energy range, growth of surface radiation defects was strongly dependent on the nature of target and laser energy. At 0.6-1.0 joules, the target structure was predominantly band-like; but melting zones and craters did not appear. Individual 150-200 μ microcraters were formed however on the surface due to the intensive laser pulse peaks. With an increase of energy to 2 joules, the structure band disappeared and macrocrater and melting zones were observed on the target. The macrocraters were almost identical, nearly circular and their size was a function of target type, varying between 800 and 1050 μ. For W, Mo, Ni, and Zn targets, macrocraters attained 800, 1050, 950, and 1200μ respectively, at a laser energy of 2 joules. Iou current variations were recorded by an

oscillograph in synchronism with the laser pulse to determine the defect formation rate, energy absorption and changes in crater structure with time. Typical oscillograms of ruby laser pulsed radiation at 0.6 and 2 joules and simultaneously obtained pulsed ion current with a tungsten target are shown in Fig. 1.

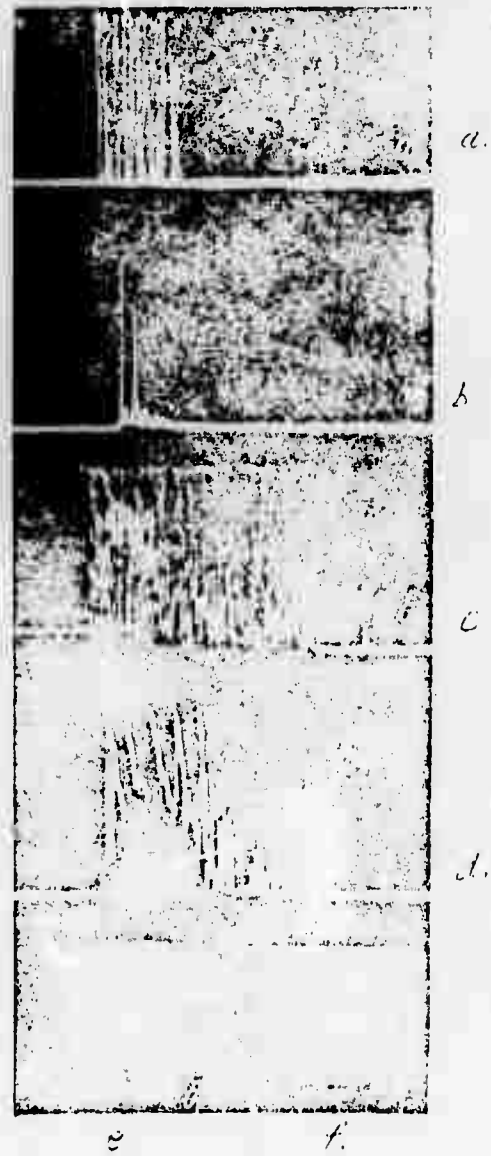

Fig. 1. Oscillograms of laser radiation at 0.6 joule (a), and 2 joules (c); ion currents of W target at 0.6 joule (b) and 2 joules (d); and defects formed on the surface of W target at 0.6 joule (e) and at 2 joules (f).

From the oscillographic results, the authors conclude that at low laser energies, ion currents assume a peaking character, are short in duration, occur after the start of the laser pulse, and are possibly connected with the formation of band structures and microcraters; at higher

energies, ion currents have a quasi-continuous character, and increase in duration and amplitude, which is related to formation of craters and melting zones.

IX. EXPLODING WIRES

Dolmatov, K. I. Current break during electric explosion of a wire, IAN Uzb SSR, Ser. fiz.-mat. nauk, no. 1, 1972, 97-98.

Characteristics of a current break were studied experimentally for discharge of two capacitors across a thin tungsten or molybdenum wire. Current intensity was determined by measuring voltage across a 0.0198 ohm resistance in the circuit. Duration τ of the current break was measured as a function of discharge potential U , and wire length l, diameter d, mass m, and resistance R. The experimental plots show that τ rapidly decreases with an increase of U from 1 to 3 kv for 15 mm. tungsten wires of 0.129 - 0.200 mm. dia. and 40 mm. molybdenum wires of 0.10 - 0.80 mm. dia. In contrast, at a constant U = 2.5 or 3 kv, τ increases with increased l and attains a very high value with a sufficiently long wire. To assess the effects of increased m and R simultaneous with an increase in f, W and Mo wires of varying m and R = 2.8 and 0.449 ohm, respectively, were exploded. The experimental plots reveal that τ is directly proportional to m, i.e., τ = 750 m for W and 2,250 m for Mo. Wires of different R, but a constant m = 60.36×10^{-4} for W and 15.76×10^{-4} g for Mo, were also exploded (Fig. 1).

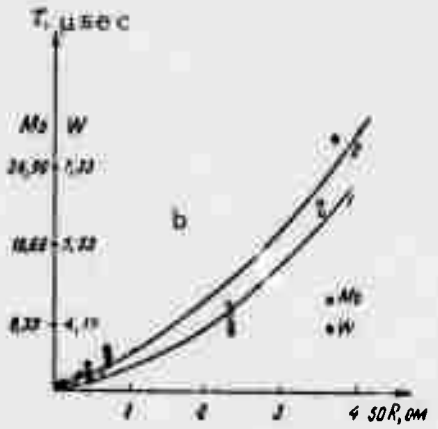

Fig. 1. Experimental τ (R) plots of W and Mo exploding wires

The experimental results were in agreement with the theory of current break by micro-disruptions in wire material.

X. ELECTRICAL DISCHARGES

Trubnikov, B. A. Nature of ball lightning. DAN SSSR, v. 203, no. 6, 1972, 1296-1298.

In an attempt to clarify the origin of the alleged 10 - 20 cm radio waves in lightning discharges, the author introduces modifications to the Dawson-Jones model of ball lightning. (Pure and Appl. Geophys., v. 75, 247, 1969). The principal modification assumes that the cavity which is hypothetically formed in the channel of ordinary straight lightning, is filled with radiation of characteristic wavelength in the millimeter or sub-millimeter range. This assumption is based on the so-called "ionosphere effect" on radio wave formation and propagation in the lightning channel. The plasma frequency ω_0 in the sheath around the channel increases by multiple discharges of lightning to a value corresponding to submillimeter wavelengths in vacuum. The waves of a frequency $\omega < \omega_0$ from the channel cannot penetrate the plasma and are therefore reflected. Powerful radio waves of a frequency $\omega < \omega_0$ consequently accumulate progressively in the space surrounded by the plasma sheath and propagate along the lightning channel. The proposed model of ball lightning formation (Fig. 1) comprises three successive stages. In the first stage,

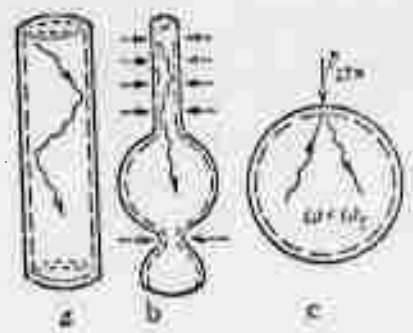

Fig. 1. Ball lightning formation model

(Fig. 1a), electron density in a cylindrical discharge (Z-pinch) increases, i.e., a "light lock" is formed, in a channel constriction. In the next stage (Fig. 1b), a pear-shaped bulge is formed above the constriction by radiation emitted from the compressed upper channel. In rare cases, the bulge may expand by radiation pressure from above to a ball (Fig. 1c), which is sustained by intense oscillations in the cavity, even after the main discharge ceases. In contrast to the Dawson-Jones hypothesis, the horizontal propagation of ball lightning is here explained by its preferential repulsion from the ball's hot trail of free electrons. The same effect may counterbalance the buoyancy force. The radiation pressure in the sphere must exceed atmospheric pressure; hence the total stored energy could be higher than in the Dawson-Jones model. This hypothesis is supported by the hypothetical structure of the plasma sheath (Fig. 2).

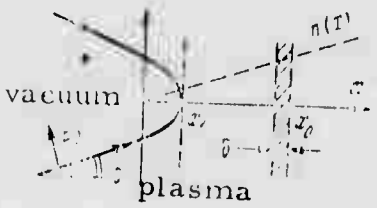

Fig. 2. Hypothetical model of plasma sheath around a ball lightning cavity

The wave field at the point x_o, with an estimated amplitude $E_x > E_o$ of the incident wave and concentrated in a very narrow slit δ is presumably capable of creating a thin shield which protects the cavity from the external neutral gas flux. Ionization of neutral molecules in the slit and their ejection by electrodynamic forces may increase external pressure, and the energy content of the cavity.

Pryadkin, K. K., R. V. Mitin, and N. N. Klimov. Electrodeless discharge in xenon at pressures to 40 atm. IN: Fizika plazmy i problemy upravlyayemogo termoyadernogo sinteza. Kiyev. Izd-vo Naukova dumka, no. 1, 1971, 226-230.

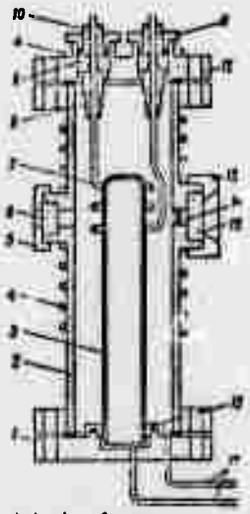

Fig. 1. Sketch of discharge chamber with external support. 1 - lower flange; 2 - stable metallic chamber; 3 - quartz tube; 4 - cooling coil; 5 , 11, 13 - nut; 6, 15 - observation ports; 7 - HF generator; 8 - teflon seal; 9 - quartz seal; 10 - teflon insulator; 12 - upper flange; 14 - projection camera; 16 - tightening ring; 17 - connection pipe.

Electrodeless high-frequency discharges in xenon at pressures to 40 atm were studied and the possibility of generating such discharges at still higher pressures was demonstrated. A fractional radiant energy loss in the overall discharge energy balance was determined as a function of discharge power and chamber pressure within the interval of 0.1 - to 40 atm. The maximum radiated power achieved at pressures of 5 to 40 atm was about 3.5 kw and the maximum light flux was about $1.5 \cdot 10^5$ l. Two discharge chamber structures were used: a thick-walled quartz chamber cooled by air or water, and a water-cooled chamber with an external support, illustrated in Fig. 1. Experimental procedures are outlined and results are plotted.

XI. PLASMA DYNAMICS

Petrenko, V. I., R. V. Mitin, Yu. R. Knyazev, and A. V. Zvyagintsev. High-current pulsed arc in hydrogen at pressures to 400 atmospheres. IN: Fizika plasmy i problemy upravlyayemogo termoyadernogo sinteza. Kiyev, izd-vo Naukova dumka, no. 1, 1971, 205-212.

Experiments in initiating a high pressure pulsed discharge in hydrogen to generate and investigate properties of a dense hydrogen plasma are discussed. The experimental device comprised a high-pressure discharge chamber, a thermo-compressor and condenser batteries. The discharge chamber was a thick-walled cylindrical metal vessel, designed for a maximum operating pressure of 1000 atm. The chamber had three diagnostic windows for conducting optical, photographic and other observations; chamber gas volume was about 1 liter. The thermocompressor maintained the required system pressure, and a liquid nitrogen coolant ensured a chamber hydrogen pressure of 500 atm. The pulsed discharge was initiated using a 0.7 mm copper wire between electrodes fitted with tungsten terminals as shown in Fig. 1. The condenser

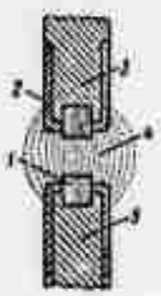

Fig. 1. Discharge configuration

1 - tungsten inserts; 2 - textolite cap; 3, 5 - electrodes; 4 - plasma

battery, with a capacitance of 8000 μf, was discharged through the conductor wire establishing an operating voltage of 2.5-3kv. Arc current was about 60 - 70 ka, with a pulse duration of 0.6 msec and a stable arc length up to 20 mm. The electrical characteristics of the pulsed hydrogen arc were studied and the visible brightness was measured. The plasma parameters analysis shows that a dense plasma is formed during pulsed discharges in hydrogen at pressures of 400 atm and currents of about 65 ka. This plasma has a charged particle density of about $10^{19} cw^{-3}$ and a temperature of about 18,000 ^{o}K. Typical pulse wave forms and dynamic volt-ampere characteristics of the discharge are also shown.

Kaliski, S. Cumulation of plasma and magnetic field during explosion of a heavy conductive shell. Biul. WAT J. Dabrowskiego, v 20, no. 11, 1971, 9-16 (RZhF, 4/72, #4G16).

The problem of combining plasma cumulation with that of the initial magnetic field during an explosion oriented toward the center of a system is treated by the method of averaging. A solution is presented to equations of plasma motion in a magnetic field and an equation of energy in plane and cylindrical systems. Using a general solution, separate boundary conditions are derived for cumulation of the magnetic field or the plasma. The description of the boundary condition of plasma cumulation alone by the method of averaging is considered meaningless, however, without allowance for additional sources (e.g. lasers, magnetic fields, and mechanical pressure) acting upon the plasma.

Kaliski, S. Cumulation of a plane electromagnetic field at relativistic initial velocities of a conductive shell. Biul. WAT J. Dabrowskiego, v. 20, no. 11, 1971, 17-23. (RZhF, 4/72, #4G7).

The problem of magnetic field cumulation during a field-oriented explosion of a heavy conductive shell is analyzed in an approximation of plane geometry. Quasi-relativistic velocities of the conductive shell were investigated (the terms of the $(v/c)^2$ order, where v is the shell velocity, are disregarded). Using the method of characteristics, Maxwell equations are solved with a boundary condition formulated by a standard differential equation which describes motion of the shell. In the particular case of $v/c \leq 1$, field cumulation is described by a well-known solution for a quasi-static state.

XII. EQUATIONS OF STATE

Pridatchenko, Yu. V., and Yu. I. Shmakov.
Rheological equations of state for weak polymer solutions with rigid ellipsoidal macromolecules.
ZhPMTF, no. 2, 1972, 125-129.

Results obtained by Shmakov and Taran (I-FZh, v. 18, no. 6, 1970) are generalized by taking macromolecular inertia and the effects of external electric and magnetic force fields into account when deriving rheological equations of state for weak polymer solutions with rigid ellipsoidal macromolecules and macromolecular Brownian motion. The effects of macromolecular inertia on the rheological properties of liquids are analyzed. Using Jeffery's expressions for flow perturbation caused by a suspended rigid ellipsoid in a viscous Newtonian fluid, the authors derive equations for the stressed state of liquid. From these, eight rheological constants are determined for equations describing the isothermal motion of an incompressible anisotropic fluid with a constant magnitude structural orientation vector. The ninth rheological constant is found by considering a special case (the absence of external force fields and a negligibly small particle inertia). Rheological equations of state are found by averaging Ericksen's tension tensors over the angular distribution function for the axis of rotation of an elliptical particle, and making use of the rheological constants. As an example, the Couette flow of a polymer solution with rigid ellipsoidal macromolecules in the absence of external force fields and rotational Brownian motion is analyzed. It is found that, in the presence of macromolecular inertia with or without macromolecular Brownian motion, weak polymer solutions of molecules, approximated by a rigid ellipsoid of rotation will exhibit non-Newtonian properties.

Zhdanov, V. A., and V. F. Konusov. On the theory of air equation of state for solids. IN: Itogi issledovaniy po fizike, 1917-1967. Tomsk. Tomskiy universitet, 1971, 87-102. (RZhKh, 10/72, no. 10B577)

Consideration is given to the general properties of equations of state derived in terms of quasi-harmonic approximations of crystal lattices under the effect of mechanical stresses of an arbitrary type. The influence of lattice symmetry on the form of the equations of state is clarified, as well as that of the binding forces. A study is made of the critical states of crystal lattices prior to mechanical failure. Results of research on a series of specific crystals are discussed.

Malyshev, V. V. Equation of state for uranium hexafluoride over a wide range of state parameters. Atomnaya energiya, v. 32, no. 4, 1972, 313.

Experimental data on saturated vapor pressure P_s, densities ρ_v and ρ_l of UF_6 vapor and liquid at equilibrium are approximated by the equations

$$\lg P_s\,(bar) = 10{,}5488 - 2344{,}4/T - 0{,}013624T + \\ + 1{,}0347\cdot 10^{-5}T^2; \qquad (1)$$

$$\rho_v\,(g/cm^3) = 1{,}369 - 0{,}2826\Theta - 0{,}0211\Theta^2 + 0{,}00503\Theta^3; \qquad (2)$$

$$\rho_l\,(g/cm^3) = 1{,}369 + 0{,}0616\Theta + 0{,}2757\Theta^2 + 0{,}09975\Theta^3 + \\ + 0{,}01677\Theta^4 - 0{,}001028\Theta^5, \qquad (3)$$

where

$$\Theta = (504{,}5 - T)^{1/3}. \qquad (4)$$

Compressibility of UF_6 was determined using a constant volume piezometer. Pressure to 242 bar, densities to 3.417 g/cm^3 and temperature in the 364 - 592°K range were measured with respective errors less than 0.1 - 0.2%, in the 0.05 - 0.13% range and 0.07°K. Equations (1), (2), and (3) describe the experimental data with an error less than 0.3% in the 364.0 - 504.5°K range, equal to 0.5% in the 403.7 - 504.5°K range, and to 0.2% in the 372.6 - 504.5° K range, respectively. The critical parameters of UF_6, namely ρ_c = 1.369 ± 0.005 g/cm^3, T_c = 504.5 ± 0.2°K, P_c = 46.0 ± 0.1 bar, and $S_c = \rho_c T_c R\mu / P_c$ = 3.55 ± 0.02, were determined from Equations (1) - (3). Heats of vaporization were calculated from the Clausins - Clapeyron equation using Equations (1) and (3) and were expressed by an approximate formula with a 1.1% error.

The UF_6 equation of state is given in the form of an interpolation polynomial of the 5th degree,

$$\frac{\pi\varphi}{\tau} = 3{,}55\left[1 + \sum_{k}\sum_{m} b_{mk}\tau^{k}\varphi^{m}\right], \qquad (5)$$

in variables $\pi = P/P_c$, $\tau = T/T_c$, and $\phi = \rho_c/\rho$. The b_{mk} values in (5) are tabulated for m = 1-5 and k = 0-4. Equation (5) describes the experimental data with a 0.2 - 0.3% error in the region of superheated vapor ($\rho \leq$ 1.4g/cm^3) and with a 1% maximum error at $\rho \leq$ 2.8g/cu.cm. Secondary virial coefficient B values are tabulated for the 463.3 - 592.2°K range. The intermolecular parameters were calculated from the Lennard-Jones (12-6) potential function. This paper is an extension of an earlier report by Malyshev on the same subject (February Monthly Report, p. 70).

XIII. PROPERTIES OF COMPOSITE MATERIALS

Shermergor, T. D., and V. N. Dolinin. Rheological characteristics of orthotropically-reinforced polymers. MP, no. 2, 1972, 276-283.

A model is developed for the rheological characteristics of orthotropically-reinforced polymers based on calculations of experimental values for elastic and rheological properties of individual components. This approach allows a drastic reduction in the number of parameters necessary for a complete specification of the anisotropy of elastic and rheological properties of composite materials. The orthotropic material is assumed to consist of anisotropic grains randomly oriented along the x-y-z axes. Each grain has a laminar structure with alternating elastic and viscoelastic layers. The degree of anisotropy and the viscoelastic properties of the composite material can be varied to a large extent by a suitable choice of ten parameters (four elastic moduli, four concentration coefficients, and two rheological characteristics). Parameters of individual components are used to compute the rheological characteristics of the composite material either in the Foygt (sic) or Royce approximation. The authors point out that Foygt's method (based on the homogeneity of the microdeformation hypothesis) is useful for the determination of operators of elasticity and shear moduli, while the Royce approximation (the homogeneity of the microtension hypothesis) gives a simplified form of Young's modulus and Poisson's coefficients. Using the Royce approximation method, pliability matrices are derived for a viscoelastic composite in operator form and operator representations of 12 technical elastic moduli. Due to the orthotropic symmetry of the material, only 9 of these are independent. It is shown that each of the elastic moduli is represented by two real or complex resolvent Q* operators. The contributions of Young's moduli components are calculated for various concentrations and anisotropies, and conditions determined for discarding one of the Q* operators. For a complex exponential Q* operator with a

fractional exponent equal to -1/2, an integral kernel representation is derived, and time dependencies of the real and imaginary parts are computed and plotted. A graphical analysis shows that the representation of an elastic modulus by a complex Q* operator assures an energy decrease with tension relaxation in agreement with the second law of thermodynamics.

Karpinos, D. M., L. I. Tuchinskiy, M. L. Gorb, E. S. Umanskiy, and V. Ya. Fefer. Mechanical properties of titanium reinforced by unidirectional molybdenum wires. Problemy prochnosti, no. 6, 1972, 28-32.

The mechanical properties of type VT 1-0 titanium, reinforced with unidirectional wires of molybdenum M4, were investigated. Reinforcement wires 0.8 mm in diameter were wound unidirectionally on titanium matrix plates 0.08 mm thick. The wire volumetric content was regulated by the winding pitch, and comprised 10, 20, 32, and 44% by volume. Tensile strength and impact viscosity tests were conducted. Non-reinforced titanium plates were tested for comparison. The tensile strength was tested at 20, 400, 600, and 800° C; five specimens for each volumetric content of the reinforcement wire were tested at each temperature. At all investigated temperatures, a practically linear relationship was observed between the short-term tensile strength and the volumetric wire content V_w. An increase of titanium strength due to reinforcement is characterized by the strengthening coefficient K, which represents the ratio of the composition strength to the titanium strength at a specific temperature.

Fig. 1 shows the effect of temperature upon the value of K at different values of V_w. Fig. 2 shows the short-term tensile strength of reinforced titanium in relation to V_w. Comparison of the results with data on the known strength of the critical wire shows that 70-75% of the initial strand strength is utilized in the composition. In all the compositions studied, V_w is above the critical value.

Reinforcement by molybdenum wire sharply decreased the titanium plasticity and at normal temperature moderately increased its tensile strength. The modulus of normal elasticity E of molybdenum-wire reinforced titanium increased linearly with V_w according to the formula:

$$E = 204\ V_w + 10,000\ kg/mm^2$$

The specific modulus of elasticity (E/specific gravity) of the composition increased with V_w. Calculations reveal that when $V_w = 61\%$, the value at which the specific gravity of the Ti-Mo composition is equal to that of steel, $E = 22,500\ kg/mm^2$, which is about 10% greater than that of steel. Impact ductility tests ($a, kg/cm^2$) were made on specimens at various angles α between the specimen axis and the direction of the reinforcing s strands. The change of a is presented in relation to angle α (Fig. 3) and E_w (Fig. 4).

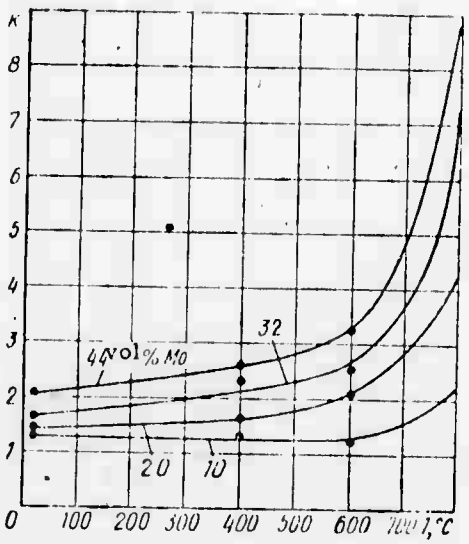

Fig. 1. Effect of temperature on strength coefficient, K.

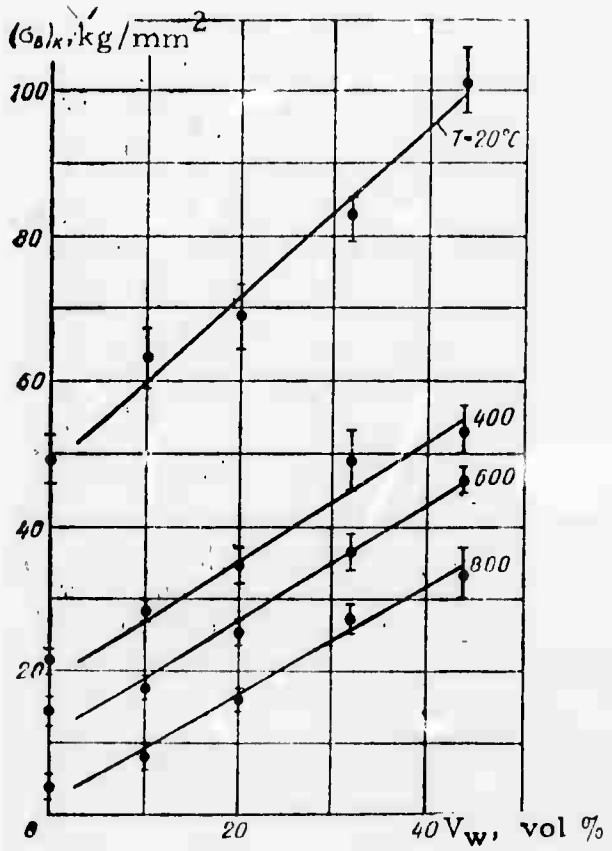

Fig. 2. Short term tensile strength of reinforced titanium.

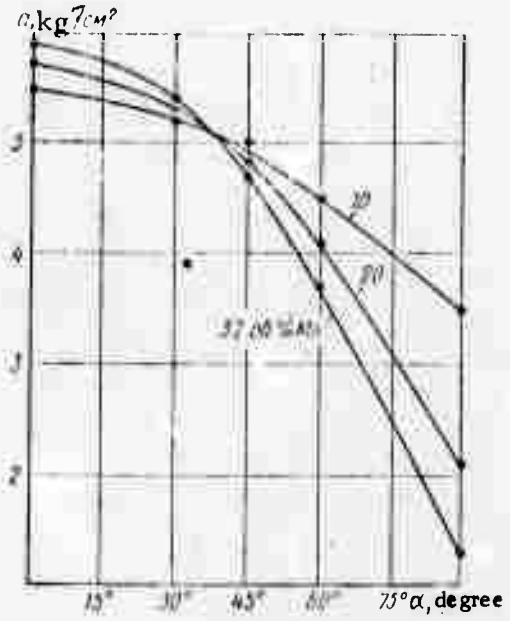

Fig. 3. Titanium impact viscosity as a function of angle, α.

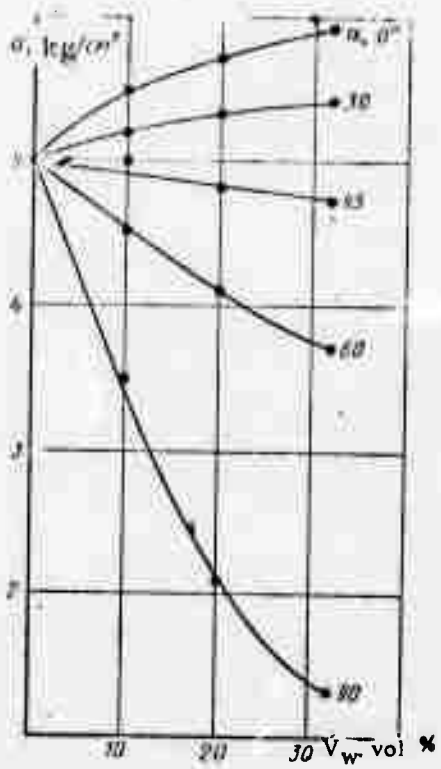

Fig. 4. Titanium impact viscosity as a function of molybdenum volumetric wire content, $E_{v.}$.

Karnozhitskiy, V. P. Experimental investigation of the stability of compressed heated three-layer plates beyond the proportionality limit. IVUZ Avia., no. 1, 1972, 128-131.

An experimental investigation was conducted to determine the applicability to the calculation of real plates of a previously proposed empirical formula for determining the critical stresses of asymmetrical plates, nonuniformly heated with respect to thickness beyond the proportionality limit. The formula is analogous to one extensively used in determining the critical stresses of single-layer plates at normal temperatures.

The top and bottom edges of the plate were simply supported. One load-bearing layer was electrically heated to 150-200°C; the other was cooled by carbon dioxide. The experimental rectangular panels consisted of load-bearing layers of equal thickness, made of the same material, glued to a honeycomb filler of AMGN material 0.05 mm thick, made of hexagonal cells, with 4.18 mm sides. Three aluminum alloys, a titanium alloy, and steel were used as materials for the load-bearing layers. The panel length (measured along the compressing force) of the 31 panels tested varied from 290 to 300 mm, and the width from 216 to 300 mm. The mean temperature of the heated load-bearing layer in various panels was alternated from 293 to 455° K, that of the cooled side from 273 to 363° K.

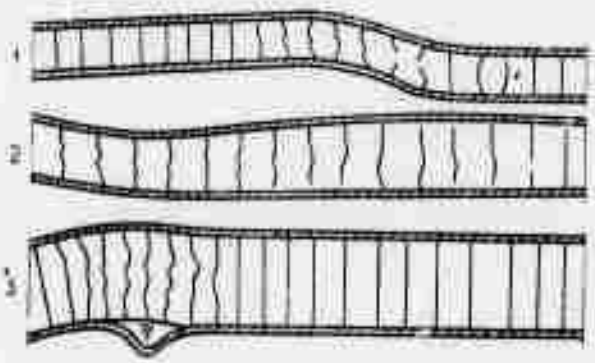

Figure 1.

Three types of panel stability loss are observed: a) Skew-symmetric buckling, when the compression stresses in the load-bearing layers attain the theoretical critical value; this takes place if the stresses at the junction point of the load-bearing layer with the filler are insufficient for detachment of this layer from the filler or for stability loss of the honeycomb walls (Figure 1, plate 1). b) Buckling with stability loss (crumpling) of the filler honeycomb, when the stresses at the junction point of the load-bearing layer with the filler attain a value which is sufficient for stability loss of the honeycomb filler (Figure 1, plate 2); the forces compressing the panel have not reached their theoretical critical value. c) Buckling with detachment of the load-carrying layer, when the stresses at the junction point of the load-bearing layer with the filler attain a value which is sufficient for detachment of the load-carrying layer from the filler (Figure1, plate 3), the forces compressing the panel have also not reached their theoretical critical value.

The conclusion is drawn that the influence of initial unevenness upon the stability of three-layer constructions with a honeycomb filler can be significant; and a theory is required for verifying the strength and stability of the honeycomb filler of compressed heated three- layer constructions with any initial unevenness, both before and beyond the proportionality limit.

When plates of the described type containing load-bearing layers of aluminum alloys no thicker than 1 mm and an initial unevenness no greater than 0.3 mm, are heated nonuniformly with respect to thickness, the critical compression stresses can be determined in a first approximation on the basis of the proposed empirical formula, with 0.85 as the experimental factor. Honeycomb cells of an aluminum alloy, or of a harder material, must have a thickness of not less than 0.05 mm and hexagonal sides not longer than 4.18 mm. Thicker load-carrying layers or greater initial unevenness will yield exaggerated results.

An additional experiment is necessary to determine the possibility of application of the empirical formula for the calculation of three-layer panels with load-bearing layers of titanium alloys and steel. When designing three-layer structures with load-bearing layers of titanium and steel, it is necessary to increase the stability of the honeycomb walls by increasing their thickness or by decreasing the dimensions of the hexagon.

Kopan', V. S., A. V. Lysenko, and V. D. Mikhalko.
Effect of surface reinforcement and the medium on properties of aluminum and tin laminated materials.
F-KhMM, no. 6, 1971, 15-17.

The purpose of this article is to establish the dependence of microviscosity limits on the specific contribution of the inner surfaces in a multilayer Al-Sn composition (MLC) and to determine possible causes of observed phenomena. The authors establish that the tensile strength of MLC depends on the average thickness of a single layer (the critical thickness is 0.1 μm) and increases with increased inner surface area. The reinforcement is explained by changes in the dislocation structure on the metal interlayer surfaces. Earlier structural studies of the boundaries between the monocrystals of different elements established the existence of an incongruity dislocation lattice acting as an effective barrier for sliding dislocations. The effectiveness of this lattice possibly increases with the increased interlayer area and has a pronounced effect on the microviscosity limits. The existence of a single critical deformation amplitude indicates that the changes of the centers of the dislocation lattice on the interlayer boundary are probable causes of the collapse of the dislocation lattice in MLC layers. Tensile stress has a tendency to increase with a decrease of individual layer thickness. Experimental durability tests of Al-Sn MLC, as a function of time exposure to humidity, show a pronounced decrease of durability with increased exposure. The changes in density and mass of a test sample are explained by interlayer boundary corrosion. Soaking of the sample in distilled water resulted in its total dissolution within 24 hours, comprising non-metallic sediments. The solubility of the sample increased as its layer thickness decreased. The above phenomena are explained by the intensive corrosive processes which take place on the interlayer boundaries.

XIV. SOIL MECHANICS

Vovk, A. A., and A. V. Mikhalyuk. Wave process characteristics in a ground mass during explosions by air-casing charges. ZhPMTF, no. 2, 1972, 105-110.

A study of the wave process characteristics in a ground mass during explosions by air-casing charges was conducted with concentrated confined charges (charge weight 0.2 kg) and linearly distributed ejection charges (4 kg of explosive per meter) in loam with a density of 1990 kg/m^3 and an average moisture content of 14.17% by weight. The effect of the charge air-casing size on the parameters of detonation waves propagating in the ground during the explosion was investigated. The explosive used in all experiments was pressed trotyl with a density of 1600 kg/m^3, a detonation rate of 6 km/sec, and a specific intrinsic energy of 1010 kcal/kg. The charge was placed in a cardboard case, with a volume exceeding the charge volume by the air casing size. The stress wave parameters were measured by a tensometric complex. Sensors were installed to permit registration of the radial σ_r, axial σ_z, and circumferential σ_q components of the stress tensor.

An analysis of the experimental results shows that when the volume of the air casings is close to optimal, an increase of the detonation impulse time in the low-pressure region occurs. This is particularly evident in explosions of linearly distributed charges. Scattering of the experimental point data precluded the drawing of conclusions on the explosions of the concentrated confined charges. Changes in stress wave parameters during the explosion of air-casing charges affect the distribution of pressure impulse values. The redistribution of the deformation energy due to changes in the charge design was confirmed by experimentally established relationships on the change with distance of the radial impulse values on the load sector at various relative volumes of the air casings during explosions of centrally-symmetric and axisymmetric charges.

It is shown that the air casing of a charge has a significant effect on practically all the parameters of a wave disturbance propagating in the ground from an explosion. The characteristic wave processes in ground masses from explosions by air-casing charges can be used for calculating explosion effects when cutting through mine workings and other underground structures in compressible soil.

Inogamov, I. I., and F. N. Pys'.
Destruction mechanism of rocks from explosions. IAN UzSSR. Ser. tekh. nauk, no. 3, 1972, 77-80.

Soviet research on the mechanism of rock destruction by explosive action is surveyed. Vlasov et al (IAN SSSR, 1962) showed that an approximate solution of explosion problems can be obtained by assuming that transmission of the explosion energy to the surrounding medium is instantaneous, and that the medium is incompressible. Principles were developed on this basis for the calculation of rock fragmentation by an explosion. The granulometric composition of the blown-up rock mass can consequently be theoretically determined by classical mechanics, and the fragmentation action of cylindrical charges can be calculated. However, the only changes and deformations taking place in the medium which can be evaluated using this model of the rock-fragmentation process, are the end results of explosive action.

Sukhanov (IN: Sbornik. Voprosy teorii razrusheniya gornykh porod vzryva. IAN SSSR, 1958) proposed a formula for taking into account the resistance of rock to separation along the lateral surface of the explosion funnel, and the passage of the gravitational forces of the rock within the funnel. Khanukayev suggested (IN: Energiya voln

napryazheniy pri razrushenii prod vzryvom, Gosgortekhizdat, 1962) that rocks be divided into three groups based on the physicomechanical properties and manner of occurrence of the destruction process (by low, medium and high acoustic rigidity). Mosinets (IAN KirgSSR, 1963) established that 75-80% of the total destruction is created in advance by stress waves propagating in the rock mass, and it is completed by the piston action of the gaseous explosion products. According to Drukovskiy and Komir (IN: Sbornik. Vzryvnoye delo, 1965) the mechanism of rock destruction from an explosion is determined by the value and duration of the explosive impulse. Mel'nikov and Marchenko (IGO AN SSSR, 1959) proposed a method for decreasing the explosion energy loss by using charges dispersed lengthwise by air intervals.

The mechanism of the action of Ignadit was reported on by Demidyuk (IN: Sbornik. Vzryvnoye delo, no. 45, 1960). The authors note in conclusion that a large number of differing and in some cases contradictory theories have been presented on explosive effects in rocks, and remain to be reconciled.

Nematov, L. Propagation of one-dimensional spherical shock waves in soil (direct problem). IN: Voprosy vycheslitel'noy i prikadnoy matematiki, Tashkent, no. 7, 1971, 115-119 (RZhMekh, 5/72, #5V501)

The problem is considered of the propagation of a shock wave formed during the expansion of a sphere, in an unbounded space. At the initial moment of time, the spherical surface instantaneously acquires a finite velocity, which then changes in accordance with a given law. The solution is worked out on a computer by the method of characteristics. The obtained values of the velocity and deformation of particles in the shock wave are presented as functions of time and space coordinates.